energies

MDPI

Article

A Binary Expansion Approach for the Water Pump Scheduling Problem in Large and High-Altitude Water Supply Systems

Denise Cariaga [1,2,*], Álvaro Lorca [1,3,†] and Miguel F. Anjos [2,4,†]

[1] Department of Industrial and Systems Engineering, Pontificia Universidad Católica de Chile, Santiago 7820436, Chile; alvarolorca@uc.cl
[2] School of Mathematics, The University of Edinburgh, Edinburgh EH9 3FD, UK; anjos@stanfordalumni.org
[3] Department of Electrical Engineering, Pontificia Universidad Católica de Chile, Santiago 7820436, Chile
[4] GERAD, HEC Montreal, Montreal, QC H3T 1N8, Canada
* Correspondence: dccariaga@uc.cl
† These authors contributed equally to this work.

Abstract: The water pump scheduling problem is an optimisation model that determines which water pumps will be turned on or off at each time period over a given time horizon for a given water supply system. This problem has received considerable attention in mining and desalination due to the high power consumption of water pumps and desalination plants and the complicated dynamics of water flows and the power market. Motivated by this, in this paper we solve the optimal operation of a desalinated water supply system consisting of interconnected tanks and pumps that transport water to high-altitude reservoirs. The optimisation of this process encounters several difficulties arising from (i) the nonlinearities of the equations for the frictional losses along the pipes and pumps, which makes the problem a nonlinear mixed-integer model, and (ii) many possible combinations of pressure head and flow rates, which quickly leads to high computational costs. These limitations prevent the problem from being solved in a reasonable computational time in high-altitude water supply systems with more than six pumps and reservoirs, as in many networks worldwide. Therefore, in this work we develop new exact methods for the optimal pump scheduling problem that use a binary expansion approach to efficiently account for the existing nonlinearities by reducing the computational difficulties of the original problem while keeping an excellent representation of the physical phenomena involved. We also extensively tested the proposed approach in different network topologies and a case study for a real-world copper mine water network, and we conclude that the binary expansion approach significantly reduces the computational time for solving the problem with high precision, which can be very relevant for the practical daily operation of real-world water supply systems.

Keywords: discrete optimisation; water supply systems; water pump scheduling problem; nonlinear optimisation

Citation: Cariaga, D.; Lorca, Á.; Anjos, M.F. A Binary Expansion Approach for the Water Pump Scheduling Problem in Large and High-Altitude Water Supply Systems. *Energies* **2024**, *17*, 4107. https://doi.org/10.3390/en17164107

Academic Editor: Helena M. Ramos

Received: 17 July 2024
Revised: 14 August 2024
Accepted: 15 August 2024
Published: 18 August 2024

1. Introduction

The optimal operation of water and energy networks is a relevant problem worldwide because it allows entities to plan better and ensure the reliability of both networks. For the water network, the operation consists of determining which water pumps will be turned on or off in each period, depending on the dynamics of electricity tariffs. Therefore, the goal is to minimise the total cost of the water supply system (WSS) while meeting the water constraints and water demands at each node. In areas with severe droughts, desalination has become a solution to supply water to communities and industries such as mining, with the optimal operation of the WSSs being crucial to provide water to the region at reasonable prices. This is particularly important if the water demand nodes are located at high altitudes, such as is the case of many mining companies around the world, and particularly in Chile [1,2], because the pumping process is energy-intensive, increasing by

approximately USD 0.5/m^3 with every 500 m of altitude. Additionally, at an altitude of 4000 m, desalinated water costs USD 4/m^3 compared to spring water at USD 0.4/m^3 in some locations [3].

Furthermore, energy costs are a significant operating expense for water utilities, with approximately 4% of the electricity used in the United States being attributed to the operation of potable water and wastewater networks [4]. In California, 19% of the state's electricity consumption is for pumping, treating, collecting, and discharging water and wastewater [5]. Therefore, optimising the operation of water networks not only offers economic benefits but also helps to reduce unnecessary use of resources and minimise the ecological impact of pollution and greenhouse gas emissions [6].

On the other hand, multiple countries have committed to achieving carbon neutrality by 2050 in the 2015 Paris Agreement for Climate Action, which means renewable energies will replace carbon-fuelled energies in the short term [7]. However, renewable energies compromise the continuity and resilience of the electrical system due to their weather dependency, so planning has become a key element in preventing shortages. Furthermore, climate change has produced severe droughts in regions where it used to rain more frequently, weakening the water supply for hydropower, crops, industry, and human consumption.

We found inspiration in the pump scheduling problem for high-altitude WSSs, particularly the cases emerging from Chilean mining through its water supply systems that provide desalinated water to each mining site. Nowadays, this industry faces a severe drought [8,9], and the location of the mining operations accentuates this phenomenon since they are typically found at high altitudes, between 600 and 4000 m above sea level [10]. In addition, due to legal and environmental restrictions that protect aquifers and national reserves, the option of extracting continental water is being increasingly reduced. In 2019, 16% of the water used in the mining industry came from the sea, and it is expected that by 2030 this will increase to 47%. Thus, according to [1], the desalinated water pump would be the second most electricity-intensive process in copper mining, with 10% of the industry's total. In addition, in the Escondida mining company's case, the impulsion system's energy requirement is four times greater than that of the desalination plant [1].

The water pump scheduling problem is hard to solve due to its non-deterministic polynomial-time-hard (NP-Hard) nature [11], leading to high computational times. This is mainly due to (i) the nonlinearities of the energy loss equations along pipes and pumps and the power used by pumps and (ii) many possible combinations of head pressure and flow [12,13]. Under this context, a challenge arises for finding a faster way to optimise the WSS scheduling while minimising the system's total costs. Therefore, the main goal is in developing new optimisation models for the operations of water supply systems, finding optimal strategies to reduce systemic costs, and ensuring the water network's reliability and resilience.

Since the 1970s, researchers have addressed various problems in water networks, including reliability [14], network expansion [15,16], pipe sizing [17], and network operations [18,19]. Optimal pump scheduling has gained attention in recent years due to the increasingly complex electricity tariff schemes and because the operating costs of pumps constitute the most significant expenditure for water organisations globally [20]. Energy utilities are providing incentives by offering cheaper electricity at low demand periods. This problem has become particularly relevant due to the use of renewable energy sources, which are often weather-dependent and may not guarantee the continuity and resilience of the electrical system.

In the past, optimal operation techniques for water distribution systems (WDSs) primarily relied on deterministic methods such as dynamic programming (DP) [21–23], hierarchical control methods [24–27], linear programming (LP) [28,29], and nonlinear programming (NLP) [30]. However, since the 1990s, metaheuristic algorithms like genetic algorithms (GAs) and simulated annealing (SA) have gained popularity due to their ability to solve nonlinear, nonconvex, and discrete problems that are difficult for deterministic methods [31,32], but they do not ensure a global optimum since they are heuristics, i.e., not

exact methods. Nevertheless, deterministic methods are now reemerging because they are more computationally efficient, making them more suitable for real-time control and other applications [33]. There is also commercial software being used to optimise the water flows in water networks, like Derceto Aquadapt [34] and EPANET [35]; however, they do not integrate the switching of the water pump to minimise the total operational costs.

Refs. [12,36] summarise the mathematical model for designing and operating a water network described in Section 2. The basic model is a nonlinear network flow problem with complicated hydraulic constraints. The goal is to operate pumps, which affect the flow and pressure of the water network. This problem is NP-hard due to its nonlinearities and nonconvexities. First, the nonlinearities are present in the relationship of the pump's pressure head with the flow and in the relation between pressure head loss and flow in pipes. Second, the nonconvexities are present in the changing flow paths in pipes and tanks and in the different discrete choices of pumps to run at a given time of the day [12,37].

The water pump scheduling problem is typically planned over a day-ahead horizon, divided into 24 h periods. This discretisation of time is a practical approach to reduce the computational costs of the scheduling problem. Additionally, demand forecasts and electricity price tariffs are usually provided in discrete time rather than in continuous time, which further supports this approach [38].

The water pump scheduling problem is a nonlinear global optimisation problem, and solving such problems is an NP-hard task [39]. One way to do so is to use spatial branch and bound algorithms. Integrating spatial branching for NLPs and mixed integer branching techniques for mixed integer linear problems (MILPs) opens the possibility of developing general-purpose algorithms that can, in principle, solve nonconvex mixed integer nonlinear problems (MINLPs) to global optimality [12,40]. The basic idea of such an algorithm is to divide the problem into subproblems iteratively and to solve (usually linear) relaxations of these. Subproblems are divided by branching on integer variables and branching on continuous ones.

In a subproblem of the branching tree, the continuous domain of some nonlinear function is divided at a certain breakpoint into two smaller domains, thus creating two new subproblems. Provided the relaxation of a nonlinear constraint becomes tighter when the domain of the corresponding nonlinear function is reduced, spatial branching gradually refines the relaxations; see Figure 1 [12]. Branching is continued until, finally, the relaxations are tight enough to provide solutions that are ϵ-feasible for the original problem.

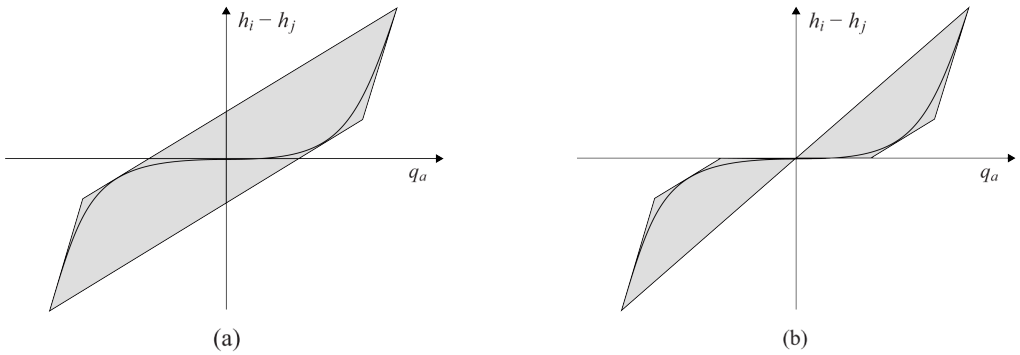

Figure 1. (**a**) Linear relaxation of the potential-flow coupling constraint. (**b**) Spatial branching refinement of the potential-flow equation in origin. Based on the work of [12].

Ref. [12] explains that a way to obtain relaxations of subproblems is to use reformulation techniques to reform all nonlinear functions into some "basic" functions. For these basic functions, linear relaxations are then readily available. The tightness of the relaxations and, thus, the algorithm's performance are highly dependent on the bounds of the domains of the nonlinearities. This fact makes efficient domain propagation between subproblems essential. Some solvers, like Gurobi, use this approach to solve nonlinear and nonconvex bilinear or quadratic problems [41]. Other solvers like Ipopt and KKT also offer nonlinear

solutions; however, they do not support mixed integer problems or do not ensure global optimality if the problem is non-convex. Therefore, they are not used in this case.

Other problems related to WSSs are the design and investment decisions to build them [42] (see Figure 2), analysis of the topological attributes of network resilience [43], the design of water networks under future demand uncertainty [44], demand response using a WSS [45–48], and operational models for the multi-product pump scheduling problem [49].

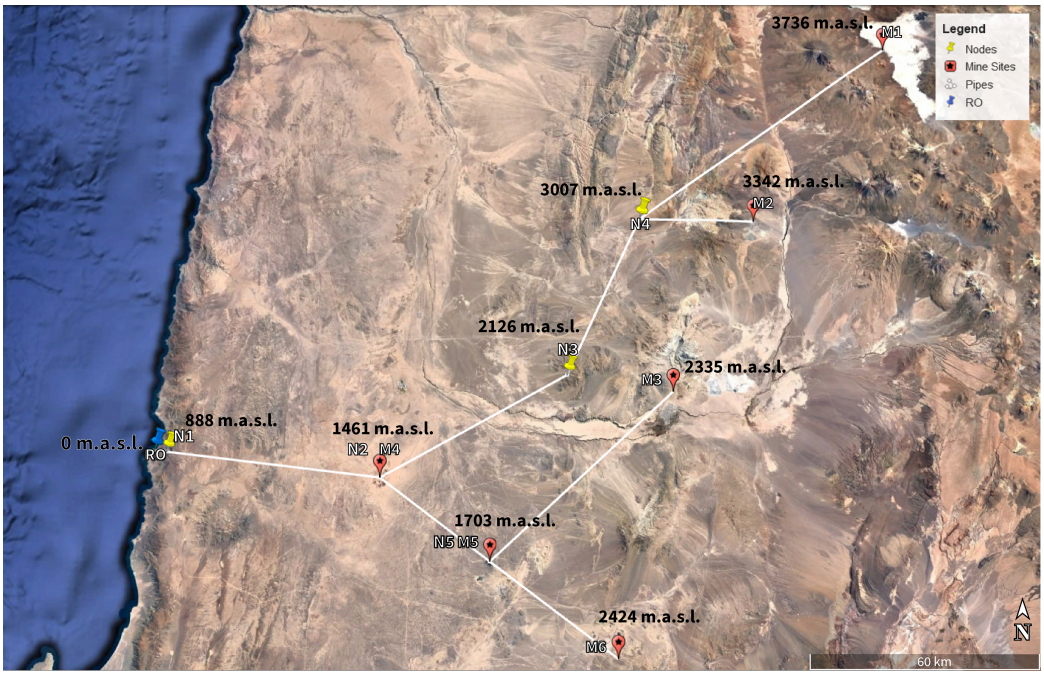

Figure 2. WSS proposed by [42] to supply six mining sites. Image made using Google Earth Pro 7.3.6.9796 (64-bit). It corresponds to the medium-size WSS used in this work.

Considering the literature reviewed above, this research identifies challenges that remain unsolved in the current state-of-the-art. The following questions summarise these challenges: How can the water pump scheduling problem for large and elevated WSSs be solved in a reasonable time? How can we efficiently represent the nonlinear nonconvex hydraulic equations in the water pump scheduling problem with desalination plants in the context of large and high-altitude water supply systems? How does a dynamic electricity tariff affect the water pump scheduling problem in high-altitude WSSs?

In this work, the main contributions are summarised as follows:

1. We optimised the water pump scheduling problem of high-altitude WSSs with multiple pumps and reservoirs using a discretised hourly time horizon and a dynamic electricity tariff. The high-altitude feature is crucial in our model since we are studying the optimal water pump scheduling for large and high-altitude water supply systems.
2. We propose a novel approach to improve the computational efficiency and allow the solutions of the water pump scheduling problem for high-altitude WSSs: the binary expansion approach. We applied this technique to the complicating hydraulic constraints of the model by partitioning some of their variables into 2^N pieces. The complicating constraints are nonlinear and nonconvex, thus making the problem hard to solve. With the binary expansion approach, we reduce computational times while keeping the optimality gap below 1% for large case studies.
3. We analysed the different models proposed in the literature to solve the water pump scheduling problem and compared them with the proposed approach in a 24 h time horizon. We also studied different WSS topologies and boundary conditions, such as the initial water level in tanks, the altitude of the nodes, the total pipe length, seasonal electricity prices, and comparison with the mining company's energy and water poli-

cies, to study the economic and computational impact of using the binary expansion approach. The WSSs utilised have heights of over 3000 m, and the networks include up to 15 water pumps. Our results show the effectiveness of the proposed approach in solving the problem and further demonstrate how a specific representation of the complicating constraints impacts the computational time of the water network operational model.

The remainder of this paper is organised as follows. Section 2 introduces the WSS operational model and its nonlinearities. Section 3 presents three proposed models, including the binary expansion approach. Following this, in Section 4 we evaluate the performance of the models using different WSS topologies based on the Chilean geography as a case study. Finally, concluding remarks are provided in Section 5.

2. Operational Model for WSSs

This section presents the operational model for the water pump scheduling problem. We introduce the operational constraints for flow, pressure, pipes, pumps, and tanks. Some of the operational equations have a nonlinear and nonconvex nature, so in Section 3 we propose different approaches to handle the computational challenge produced by these constraints.

The decisions of this problem are binary variables that determine the water pump status and continuous variables associated with the water flow in the WSS, the water pump power consumption, and the head pressure in each node. The uncertain nature of this problem is related to the stochastic hydro inflows. Therefore, the main goal of this problem is to find the optimal water pump scheduling as the power prices change over time while minimising the total operational cost of the WSS.

The WSS is formulated as a directed acyclic graph (DAG), $G = (N, A)$, with nodes, N, and arcs, A. Nodes can be categorised as junctions, $j \in J$, reservoirs, $j \in R$, tanks, $j \in S$, or desalination plants, $j \in RO$; that is, $N = J \cup R \cup S \cup RO$. Arcs can be pipes, $a \in Pi$, or pumps, $a \in Pu$; that is, $A = Pi \cup Pu$.

This article's main distinction between tanks and reservoirs is that tanks allow bidirectional flow, whereas reservoirs model the water supply source (i.e., mine water source). Tanks are normally modelled as nodes, like in this paper, but can also be treated as arcs [36]. The WSS in this paper's case study works as follows: First, the water is desalinated and then pumped into elevated tanks to continue its way up to meet the demand at different nodes. Taking into account the speed and design of these WSSs, the flow reaches a quasi-stationary status. This model also assumes that the pipes have a soft starter and finish or a frequency converter with a kind of slow slope to ensure a smooth transition of the flow; however, the design of the pipe is not considered in the modelling to simplify the calculation. Thus, there is no need to add partial differential equations to the model, and the following equations model the physical phenomena of the water pump scheduling model for a WSS.

The operational nature of the problem introduces time to the variables and parameters. In principle, time is continuous, $t \in [0, T] \subset \mathbb{R}$; however, for the model tractability it is discretised in $t \in \{1, \ldots, T\}$ periods of length $\tau \in \{\tau_1, \ldots, \tau_T\}$. Refs [12,38] point out that the time discretisation has the practical motivation that electricity demand and prices forecast are usually given in discrete and not continuous time. In this paper, the planning horizon is one day, divided into 24 hourly periods.

We made the following assumptions for this model: (i) pump start/stop can be performed instantly without any time delay; (ii) the fluid is considered incompressible, and changes in volume due to flow through pumps and pipelines can be disregarded; (iii) the fluid's physical properties remain constant, and variations in temperature and pressure are not taken into account. Pressure distribution along the pipeline is calculated assuming a steady-state process, and any effects of fluid transients in the pipeline are neglected.

2.1. Flow and Pressure

2.1.1. Conservation Equations

A positive flow, $q_{i,j,t}$, on an arc (i,j) means that it goes from i to j at time $t \in T$, while a negative value of $q_{i,j,t}$ stands for a flow of amount $\left|q_{i,j,t}\right|$ from j to i. It is possible to allow only positive flow values and account for the directions with a binary variable. Since this is a network, the flow conservation constraint applies for each node $i \in \mathcal{N}$, the difference between the sum of the pipe flows entering and exiting is equal to the water demand $d_{i,t}$ at the node at time t. Assuming that the demand must be satisfied at every time, the linear conservation constraint for every node i that is not a tank S is:

$$\sum_{j:(j,i)\in A} q_{i,j,t} - \sum_{j:(i,j)\in A} q_{i,j,t} \geq d_{i,t} \qquad \forall i \in N \setminus S,\ \forall t \in T. \tag{1}$$

Note that, for this problem, for the nodes where desalination plants are, the water flow demand is negative since it is a water input to the network. On the other hand, for mining site nodes, the demand is positive since it corresponds to the water output of the network. Finally, all the nodes in between that are not tanks have either a positive or a zero demand.

2.1.2. Flow Bounds

The absolute value of the flow is bounded due to the capacity of the arcs. This bound depends on the pipe's cross-sectional area and the maximum linear velocity. Refs. [12,15,42] emphasise that this parameter must not exceed a specific value to avoid a number of potential operating problems, for instance, the flow-assisted corrosion problem. Therefore, taking into account $v^{\max}_{i,j,t}$, for the maximum linear velocity that is allowed in a pipe (i,j) at time t, the maximum flow can be written [42] as

$$q^{\max}_{i,j,t} = \frac{\pi}{4} v^{\max}_{i,j,t,t} D^2_{i,j} \qquad \forall (i,j) \in A,\ \forall t \in T. \tag{2}$$

Then, the flow bounds are:

$$-q^{\max}_{i,j,t} \leq q_{i,j,t} \leq q^{\max}_{i,j,t} \qquad \forall (i,j) \in A,\ \forall t \in T, \tag{3}$$

where $D_{i,j}$ is the diameter of the pipe (i,j).

Note that, since we are working with a directed graph, the lower bound is zero:

$$0 \leq q_{i,j,t} \leq q^{\max}_{i,j,t} \qquad \forall (i,j) \in A,\ \forall t \in T. \tag{4}$$

2.1.3. Pressure

For the hydraulic head, $h_{i,t}$, $i \in N$ is the pressure value expressed dimensionally as a length in columns of water (m). In fluid dynamics, the hydraulic head is the total energy per unit weight of fluid and is the sum of the elevation head, Z_i, which is the altitude of the node i, $\bar{H}_j$, the pressure in the terminal node, j, and the pressure loss, $\phi_{i,j,t}$, in the pipeline or pump due to friction. The hydraulic head, $h_{i,t}$, and pressure loss, $\phi_{i,j,t}$, for pipes and pumps are explained in the following section. For the WSSs tested in this work, the pressure in the terminal node $\bar{H}_j$ is 0 m, under the assumption that every node receiving water has a storage tank exposed to the environment [50].

$$h_{j,t} - h_{i,t} = Z_j - Z_i + \bar{H}_j + \phi_{i,j,t} \qquad \forall (i,j) \in A,\ \forall t \in T. \tag{5}$$

The hydraulic head must stay between certain bounds to guarantee the nodes' minimum and maximum pressure levels. Normally, the node potentials are fixed at source nodes, as in the desalination plants in this work, reflecting the fact that, at sources, water is

not pressurised, but it exploits a fixed geographical height [12]. For all the other nodes, the lower bounds for the hydraulic head are:

$$h_{i,t} = Z_i \qquad \forall i \in RO,\ \forall t \in T, \tag{6a}$$

$$h_{i,t} \geq Z_i \qquad \forall i \in N \setminus RO,\ \forall t \in T. \tag{6b}$$

The bounds of the difference of the hydraulic head for pipes, pumps, and tanks are explained in the following sections.

2.2. Pipes

Energy Loss in Pipes

The arcs in a WSS represent pipes in which water is transported from one node to another. In models that do not have stationary status, the flow changes at the beginning and end of a pipe [36]. However, the flow is constant throughout the pipe since we are working with a quasi-stationary network. The fundamental equation for a pipe (i, j) is the head-loss equation, also denominated potential-flow coupling constraint in [40], that is regularly of the form

$$h_{j,t} - h_{i,t} = \Delta Z_{i,j} + \phi_{i,j,t}\left(q_{i,j,t}\right) \qquad \forall (i,j) \in Pi,\ \forall t \in T, \tag{7}$$

where $\phi_{i,j,t} : \mathbb{R} \to \mathbb{R}$ is a strictly increasing uneven function, concave on the negative half-axis of its domain and convex on the positive half-axis. The flow is not linear in arcs due to the friction modelling in the pipes. A positive flow as a function of the potential difference is strictly increasing but concave: higher flow values mean a higher influence of friction. The other way round, for the same reason, a positive potential loss as a function of the flow is strictly increasing and convex. Equation (7) is also referred to as the potential-loss equation because it describes the pressure loss along a pipe.

Explicit forms of the head-loss equation are called the Darcy–Weisbach equation,

$$\phi_{i,j,t} = \frac{\operatorname{sign}\left(q_{i,j,t}\right) q_{i,j,t}^2 8 L_{i,j} \lambda_{i,j}}{\pi^2 g D_{i,j}^5} \qquad \forall (i,j) \in Pi,\ \forall t \in T, \tag{8}$$

or the Hazen–Williams equation,

$$\phi_{i,j,t} = \frac{\operatorname{sign}\left(q_{i,j,t}\right) \left|q_{i,j,t}\right|^{1.852} 10.7 L_{i,j}}{k_{i,j}^{1.852} D_{i,j}^{4.87}} \qquad \forall (i,j) \in Pi,\ \forall t \in T. \tag{9}$$

Both formulations include constants like the gravitational acceleration, g, the pipe length, $L_{i,j}$, and the pipe material, $k_{i,j}$, roughness coefficient. The friction factor $\lambda_{i,j} = \lambda_{i,j}\left(q_{i,j,t}\right)$ depends on the Reynolds number (Re), which in turn depends on the flow in a nonlinear and continuous manner.

The friction coefficient $\lambda_{i,j}\left(v_{i,j,t}\right)$ in (8) is determined by the nature of the flow, as characterised by the value of the non-dimensional Reynolds number:

$$\mathrm{Re}_{i,j,t} = \frac{D_{i,j}}{\nu} \left|v_{i,j,t}\right| = \frac{4}{\pi \nu D_{i,j}} \left|q_{i,j,t}\right| \qquad \forall (i,j) \in Pi,\ \forall t \in T, \tag{10}$$

where ν denotes the kinematic viscosity of water ($\nu = 1.32 \times 10^{-6}$ m^2/s for 10 °C, and $\nu = 10^{-6}$ m^2/s for 20 °C) and $v_{i,j,t}$ is the average water velocity.

For laminar flow (Re $<$ 2320), the friction coefficient depends on the Reynolds number only, according to the law of Hagen–Poiseuille,

$$\frac{1}{\sqrt{\lambda^{\mathrm{HP}}}} = \frac{\mathrm{Re}\sqrt{\lambda^{\mathrm{HP}}}}{64} \iff \lambda^{\mathrm{HP}} = \frac{64}{\mathrm{Re}} \qquad \forall (i,j) \in Pi,\ \forall t \in T. \tag{11}$$

Note that the pressure loss, in this case, grows linearly with the flow rate,

$$\begin{aligned} h_{i,j,t}(q_{i,j,t}) &= \frac{64}{4|q_{i,j,t}|}\pi\nu D_{i,j}\frac{8L_{i,j}}{\pi^2 g D_{i,j}^5} q_{i,j,t}|q_{i,j,t}| \\ &= \frac{128\nu L_{i,j}}{\pi g D_{i,j}^4} q_{i,j,t} \qquad \forall (i,j) \in Pi,\ \forall t \in T. \end{aligned} \tag{12}$$

Since the graph studied in this work is directed, i.e., $q_{i,j,t} \geq 0$, the sign$\left(q_{i,j,t}\right)$ is set to 1:

$$h_{j,t} - h_{i,t} = \Delta Z_{i,j} + \frac{8L_{i,j}f}{\pi^2 g D_{i,j}^5} q_{i,j,t}^2 \qquad \forall (i,j) \in Pi,\ \forall t \in T, \tag{13}$$

where f is the Darcy friction factor.

Note that if the final node j is a tank, then $\Delta Z_{i,j} = \Delta Z_{i,j} + \bar{h}_j$ includes the tank height.

For future work, additional analysis could be incorporated, such as examining the impact of rust and deposits that may disrupt water flow. This effect could be investigated either as an energy loss due to turbulence within the constraints or by introducing a pipe maintenance cost penalty in the objective function.

2.3. Pumps

In pressurised networks, like the one we are working on in this paper, water flows from points of high to low pressure. Hence, increasing the pressure at certain parts of the network is necessary. For this purpose, pumps are used to raise the pressure inside a water supply network. To represent the status of the pumps, we introduce a binary variable, $x_{i,j,t} \in 0,1$, which indicates if pump $(i,j) \in Pu$ is active or shut down at time $t \in T$. Active pumps increase the hydraulic head by some controlled non-negative amount, as represented by the characteristic pump curve (Figure 3):

$$h_{j,t} - h_{i,t} = \alpha_{i,j} - \beta_{i,j} q_{i,j,t}^{\gamma_{i,j}} \qquad \forall (i,j) \in Pu,\ \forall t \in T, \tag{14}$$

where $\alpha_{i,j} > 0$ is the maximum possible pressure increase of the pump ($\Delta Z_{i,j}$), and $\beta_{i,j} > 0$ and $\gamma_{i,j} \geq 1$ are pump-specific efficiency parameters [36].

2.3.1. Energy Loss in Pumps

As pumps behave like pipes regarding the energy loss and since the graph studied in this work is a DAG, i.e., $q_a \geq 0$, and $x_a \in \{0,1\}$ indicates the state of the water pump, then the Darcy–Weisback equation and the linear Equation (14) with $\gamma_{i,j} = 1$ are:

$$\underline{M}(1 - x_{i,j,t}) \leq h_{j,t} - h_{i,t} - \left(\Delta Z_{i,j} - \frac{8L_{i,j}f}{\pi^2 g D_{i,j}^5} q_{i,j,t}^2\right) \leq \overline{M}(1 - x_{i,j,t}) \qquad \forall (i,j) \in Pu,\ \forall t \in T, \tag{15a}$$

$$\underline{M}(1 - x_{i,j,t}) \leq h_{j,t} - h_{i,t} - \left(\Delta Z_{i,j} - \beta_{i,j} q_{i,j,t}\right) \leq \overline{M}(1 - x_{i,j,t}) \qquad \forall (i,j) \in Pu,\ \forall t \in T, \tag{15b}$$

$$q_{i,j,t}^{min} x_{i,j,t} \leq q_{i,j,t} \leq q_{i,j,t}^{max} x_{i,j,t} \qquad \forall (i,j) \in Pu,\ \forall t \in T \tag{16}$$

where f is the Darcy friction factor and $\underline{M} = h_j^{min} - h_i^{max}$ and $\overline{M} = h_j^{max} - h_i^{min}$ [36].

Normally, Equation (15b) is one of the most common approaches used for the pump head loss. It is derived from (14) with the quadratic term $\gamma_{i,j} = 2$. However, the coefficient in front of the quadratic term is usually small and negative [51]. Therefore, as in [48,52], we neglect the quadratic term since its contribution is small compared to the linear term, and we approximate the pump hydraulic function with energy loss as described in (15b).

Note that (16) is the linking constraint between the binary variable $x_{i,j,t}$ and the flow $q_{i,j,t}$, where if the water pump is shut down, that is $x_{i,j,t} = 0$ and $q_{i,j,t} = 0$, the pressure difference $h_j - h_i$ is arbitrary. The value of $q^{min}_{i,j,t} > 0$ is the minimal relevant non-zero flow. Therefore, a flow of less than $q^{min}_{i,j,t}$ implies that the pump is inactive ($x_{i,j,t} = 0$), and a positive flow of more than $q^{min}_{i,j,t}$ makes the pump active ($x_{i,j,t} = 1$).

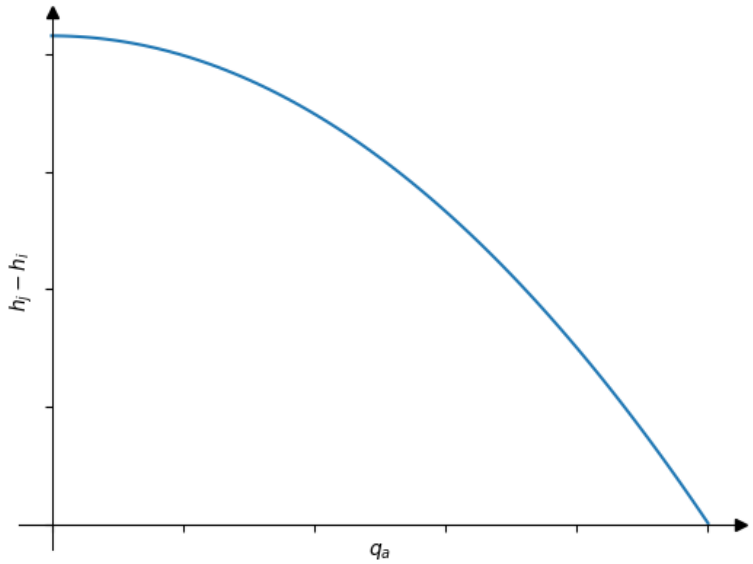

Figure 3. Characteristic curve for the pump energy loss.

2.3.2. Pump Power

For a pump with η being the combined efficiency of the pump and prime mover and ρ being the water density, its power consumption (MINLP) is a function of its head gain and water flow rate in MW:

$$P_{i,j,t} = \frac{\rho\, g}{\eta} q_{i,j,t}\, (h_{j,t} - h_{i,t})\, 10^{-6} \qquad \forall (i,j) \in Pu,\ \forall t \in T. \tag{17}$$

2.4. Tanks

Tanks can make the operation of the network more flexible. In a dynamic setting, where the demand at consumer nodes can vary over time, water can be stored in a tank during a period of low demand and extracted from it to satisfy peak demands.

$$\sum_{j:(j,i)\in A} q_{i,j,t} - \sum_{j:(i,j)\in A} q_{i,j,t} = e_{i,t} \qquad \forall i \in S \cup R,\ \forall t \in T-1, \tag{18}$$

$$e^t_i = \frac{1}{\tau_t}(h_{i,t+1} - h_{i,t}) A_i \qquad \forall i \in S \cup R,\ \forall t \in T-1, \tag{19}$$

$$h_{i,t} \le Z_i + \bar{h}_i, \qquad \forall i \in S \cup R,\ \forall t \in T, \tag{20}$$

$$h_{i,t} \ge Z_i + \bar{h}_i \gamma^{min}_i, \qquad \forall i \in R,\ \forall t \in T, \tag{21}$$

$$h_{i,1} \leq h_{i,T} = Z_i + \bar{h}_i \gamma_i \qquad \forall i \in S \tag{22}$$

with e_i^n denoting the variable volumetric tank inflow, A_i being the cross-sectional area of the tank, τ_t is a time scalar, $\bar{h}_i$ is the tank height, γ_i is the initial and final percentage of the water tank level, and γ_i^{min} is the minimum water tank level percentage during the operation. Equations (18) and (19) represent the water flow balance in a tank, which depends on its volume. To bound the maximum pressure measure in the altitude of the tanks, and since they do not allow water overflow and they are open, we need Equation (20). Usually, Equation (21) is used to set the minimum water level of a tank or reservoir during the pump scheduling operation, especially if the water operator requires a conservative volume reserved in the tank or reservoir to supply the industry in case of an energy shortage or any event that would stop the water supply for a few hours or days. Industries normally require this constraint because the cost of stopping their operation due to water shortage can cost millions every hour. Finally, Equation (22) is used to set the initial value equal to the previous day's final.

2.5. Reservoirs

As we explained before, the main difference between tanks and reservoirs is that tanks allow bidirectional flow, whereas reservoirs model the water supply source. Without loss of generality, we assume that reservoirs are infinite sources of water and that the pressure head at each reservoir, $r \in R$, is zero; in other words, the total head at the reservoir, r, only represents the elevation head [39]. Normally, reservoirs are fed by natural sources, like rivers or glaciers; therefore, it is assumed that they have an infinite supply. In this work, the "reservoirs" are, in fact, big tanks since they are located next to the mining site and they are only supplied by the desalinated WSS. Hence, they allow bidirectional flow.

2.6. Objective Function

The objective function seeks to minimise the cost of operation and the on/off penalty of the water pumps. Let X be the space of all the optimisation variables of the problem, and $T = 25$ h to adjust the 24 h cycle; therefore, the objective function is:

$$f(X) = \sum_{(i,j) \in Pu} \sum_{t=1}^{T-1} \left(P_{i,j,t} C_t + |x_{i,j,t+1} - x_{i,j,t}| C_s \right), \tag{23}$$

where C_t is the cost of electricity in having a pump on during time t, and C_s is the penalty for a single pump switch. The value of C_s is based on recommendations by [20], which consist of iterating over different values of C_s and picking one that is reasonable for the electricity prices and that allows the switching of the pumps. This is in case there is no data for the future pumping station maintenance costs.

Note that pump switching can negatively affect a system's maintenance cost due to the changing loads contributing to fatigue-related failures [45]. Hence, penalising pump switching often reduces this negative impact and accounts for maintenance costs [53,54].

Another way to represent the pump maintenance penalty is by using a quadratic term instead of the absolute value: $\sum_{(i,j) \in Pu} \sum_{t=1}^{T-1} (x_{i,j,t+1} - x_{i,j,t})^2$ [55]. Both approaches are equivalent and nonlinear; however, the absolute value has fewer added constraints in the exact reformulation, which we explain in the next section.

2.7. Water Pump Scheduling Problem

Therefore, the optimisation model for the water pump scheduling problem is the following:

$$\begin{aligned} \min \quad & (23) \\ \text{s.t.} \quad & (1), (2), (4), (6), (13), (15b), (16), (17), (18), (19), (20), (21), (22) \end{aligned} \tag{24}$$

3. Alternative Models for the WSS Operation

This section presents three methodologies to handle the nonlinearities present in the original problem, as we explained in Section 2, whose main differences lie in the final nature of the model, linear or nonlinear. We describe the three proposed models: the fixed flow model, the semi-linear model, and the binary expansion approach model. Additionally, we discuss the theoretical and practical advantages and disadvantages of each model, and we compare them using computational experiments in Section 4.

3.1. Reformulation Techniques to Solve the Complicating Constraints

To handle the complicating nonlinear and nonconvex constraints, we consider the following reformulation techniques:

1. **Fixing flow to its upper bound:** Note that Equations (13) and (15a) can become MILP if the quadratic element q_a^2 is replaced with its upper bound $(q_a^{max})^2$. The reason for fixing this value is that almost all the optimal solutions return q_a with its maximum value. Therefore, the energy loss constraint for pipes (25) and pumps (26) are:

$$h_{j,t} - h_{it} = \Delta Z_{i,j} + \frac{8L_{i,j}f}{\pi^2 g D_{i,j}^5}(q_{i,j,t}^{max})^2 \qquad \forall (i,j) \in Pi,\ \forall t \in T, \tag{25}$$

$$\underline{M}(1 - x_{i,j,t}) \leq h_{j,t} - h_{i,t} - \left(\Delta Z_{i,j} - \frac{8L_{i,j}f}{\pi^2 g D_{i,j}^5}(q_{i,j,t}^{max})^2\right) \leq \overline{M}(1 - x_{i,j,t}) \qquad \forall (i,j) \in Pu,\ \forall t \in T, \tag{26a}$$

$$\underline{M}(1 - x_{i,j,t}) \leq h_{j,t} - h_{i,t} - \left(\Delta Z_{i,j} - \beta_{i,j}\, q_{i,j,t}\right) \leq \overline{M}(1 - x_{i,j,t}) \qquad \forall (i,j) \in Pu,\ \forall t \in T. \tag{26b}$$

Note that, although (26a) could be used, (26b) is more common for energy loss in pumps. We rewrite (26b); however, it is the same as the original (15b).

2. **Reformulating the binary and continuous products:** We use an auxiliary variable, z, to linearise $z = x \cdot y$, where x is binary and y is a continuous variable such that $y \in [0, b]$. The following formulation is applied:

$$z \leq y, \quad z \leq x \cdot b, \quad z \geq y + b \cdot (x - 1). \tag{27}$$

3. **Reformulating the absolute value of binary variables:** We use an auxiliary variable, w, to linearise $w = |x - y|$, where x and y are binary variables. An analogous expression for w is $w = |x - y| = \max\{x - y, y - x\}$; therefore, the following formulation is applied:

$$w \geq x - y, \quad w \geq y - x. \tag{28}$$

Note that the reformulation for the quadratic expression for binary variables $w = (x - y)^2 = x - 2xy + y = x - 2z + y$, with $z = xy$, is similar to (27), with $b = 1$:

$$z \leq y, \quad z \leq x, \quad z \geq y + x - 1, \tag{29}$$

Nevertheless, it adds $|Pu| \times |T|$ more constraints than the absolute value reformulation (28) for the pump maintenance penalty in the objective function (23).
Using expression (28) for the pump maintenance penalty in the objective function $f(X)$ with $B_{i,j,t} = |x_{i,j,t+1} - x_{i,j,t}|$:

$$f'(X) = \sum_{(i,j) \in Pu} \sum_{t=1}^{T-1} \left(P_{i,j,t} C_t + B_{i,j,t} C_s\right), \tag{30}$$

and adding the constraints:

$$B_{i,j,t} \geq x_{i,j,t+1} - x_{i,j,t} \qquad \forall (i,j) \in Pu,\ \forall t \in \{1, \ldots, T-1\}, \tag{31a}$$

$$B_{i,j,t} \geq -(x_{i,j,t+1} - x_{i,j,t}) \qquad \forall (i,j) \in Pu,\ \forall t \in \{1, \ldots, T-1\}, \tag{31b}$$

4. **Binary expansion approach:** We discretise a continuous variable, $x \in [x_{LB}, x_{UB}]$ [56,57]:

$$x = x_{LB} + \frac{x_{UB} - x_{LB}}{2^N - 1} \cdot \sum_{i=1}^{N} 2^{i-1} \cdot x_i, \tag{32}$$

where x_i is the binary variable that determines the values of the binary division of x. The binary expansion approach for the water flow variable, $q_{i,j,t}$, is:

$$q_{i,j,t} = \frac{q_{i,j,t}^{max}}{2^K - 1} \sum_{l=1}^{K} 2^{l-1}\, q_{l,i,j,t} \quad \forall (i,j) \in A,\ \forall t \in T. \tag{33}$$

The same approach can be applied to the product of continuous variables using the binary expansion approach in one of the variables, and the other variable is left as it is. Then, we have the product of a binary and continuous variable; therefore, we can apply (27). Therefore, to linearise the bilinear product $x \cdot y$, we define the variable $z_i = x_i \cdot y$, and use (27) with a Big M:

$$x \cdot y = x_{LB} \cdot y + \frac{x_{UB} - x_{LB}}{2^N - 1} \sum_{i=1}^{N} 2^{i-1}\, z_i, \tag{34a}$$

$$0 \le y - z_i \le M\,(1 - x_i) \qquad \forall i \in N, \tag{34b}$$

$$0 \le z_i \le M\, x_i \qquad \forall i \in N. \tag{34c}$$

Applying the reformulation to the energy loss constraint in pipes (13) using $z_{k,i,j,t} = q_{k,i,j,t} \cdot q_{i,j,t}$, with $q_{k,i,j,t}$ being the binary variable for the partition of $q_{i,j,t}$ and $q_{LB} = 0$, $M = q_{UB} = q_{i,j,t}^{max}$, and (33), then the energy loss in pipes is:

$$h_{j,t} - h_{i,t} = \Delta Z_{i,j} + \frac{8 L_{i,j} f}{\pi^2 g} \frac{q_{i,j,t}^{max}}{2^K - 1} \sum_{k=1}^{K} 2^{k-1}\, z_{k,i,j,t} \qquad \forall (i,j) \in Pi,\ \forall t \in T, \tag{35a}$$

$$0 \le \frac{q_{i,j,t}^{max}}{2^K - 1} \sum_{l=1}^{K} 2^{l-1}\, q_{l,i,j,t} - z_{k,i,j,t} \le q_{i,j,t}^{max} \left(1 - q_{k,i,j,t}\right) \qquad \forall k \in N,\ \forall (i,j) \in Pi,\ \forall t \in T, \tag{35b}$$

$$0 \le z_{k,i,j,t} \le q_{i,j,t}^{max}\, q_{k,i,j,t} \qquad \forall k \in N,\ \forall (i,j) \in Pi,\ \forall t \in T, \tag{35c}$$

Similarly, as in (32), we apply the binary expansion approach to the linear energy loss constraint in pumps (15b), and in all the other constraints that have $q_{i,j,t}$, using (33):

$$\underline{M}(1 - x_{i,j,t}) \le h_{j,t} - h_{i,t} - \left(\Delta Z_{i,j} - \beta_{i,j} \frac{q_{i,j,t}^{max}}{2^K - 1} \sum_{l=1}^{K} 2^{l-1}\, q_{l,i,j,t}\right) \le \overline{M}(1 - x_{i,j,t}) \quad \forall (i,j) \in Pu,\ \forall t \in T \tag{36}$$

We also apply the binary expansion approach (34) to the pump power constraint (17) using $p_{k,i,j,t} = q_{k,i,j,t}\,(h_{j,t} - h_{i,t})$ and $q_{LB} = 0$, $q_{UB} = q_{i,j,t}^{max}$, and $M = \max\{Z_i, Z_j\}$:

$$P_{i,j,t} = \frac{\rho\, g}{\eta} \frac{q_{i,j,t}^{max}}{2^N - 1} \sum_{k=1}^{N} 2^{k-1}\, p_{k,i,j,t}\, 10^{-6} \qquad \forall (i,j) \in Pi,\ \forall t \in T, \tag{37a}$$

$$0 \le h_{j,t} - h_{i,t} - p_{k,i,j,t} \le \max\{Z_i, Z_j\} \left(1 - q_{k,i,j,t}\right) \qquad \forall k \in N,\ \forall (i,j) \in Pi,\ \forall t \in T, \tag{37b}$$

$$0 \le p_{k,i,j,t} \le \max\{Z_i, Z_j\}\, q_{k,i,j,t} \qquad \forall k \in N,\ \forall (i,j) \in Pi,\ \forall t \in T. \tag{37c}$$

3.2. Alternative Models

We proposed three alternatives for the original water pump scheduling problem (24) to analyse the computational effectiveness of the binary expansion approach method compared to other classic approaches. The first approach is the fixed flow (FF), which fixes the water flow value in the energy loss complicated equation. The second approach is

the semi-linear (SL) model, which linearises the binary and continuous products in the problem's constraints. The third alternative is the binary expansion approach (BEA), which linearises the binary and continuous products and the complicating variables of water flow and pump power.

Model 1: FF (MINLP) The fixed flow model (FF) considers a fixed value for $q_{i,j,t} = q^{max}_{i,j,t}$ in (25). The approach is an upper bound for the original problem: the flow passing through the pipes is the maximum. This approach approximates the nonlinear and nonconvex constraints for the pipes' energy loss equations. This model is still MINLP because of the bilinear term in the pump power constraint. The optimisation model is:

$$\begin{aligned} \min \quad & (30) \\ \text{s.t.} \quad & (1), (2), (4), (6), (25), (15b), (16), (17), (18), (19), (20), (21), (22), (31) \end{aligned} \tag{38}$$

Model 2: SL (MINLP) The semi-linear model (SL) only linearises the binary and continuous products using the (27) technique in (23), but leaves the pump power constraint bilinear and the energy loss equation in pipes quadratic. This method removes the complexity derived from the binary product in the problem's constraints. This model is still MINLP because of the bilinear term in the pump power constraint and the quadratic water flow in the energy loss equation. The optimisation model is:

$$\begin{aligned} \min \quad & (30) \\ \text{s.t.} \quad & (1), (2), (4), (6), (13), (15b), (16), (17), (18), (19), (20), (21), (22), (31) \end{aligned} \tag{39}$$

Model 3: BEA (MILP) The binary expansion approach model (BEA) considers the linearisation of the binary and continuous products using the technique in (27), and the bilinear products and quadratic elements using the binary expansion approach (32) and (34) in all the constraints where $q_{i,j,t}$ and $P_{i,j,t}$ are present. It is worth mentioning that the computational efficiency of the binary expansion approach is highly dependent on the number of partitions, N, taken. The higher this number is, the more accurate it should be; however, it will take longer to solve. This is because 2N equations are added to the optimisation model for every constraint where this technique is used. The optimisation model is:

$$\begin{aligned} \min \quad & (30) \\ \text{s.t.} \quad & (1), (2), (4), (6), (35), (36), (16), (37), (18), (19), (20), (21), (22), (31), (33) \end{aligned} \tag{40}$$

Note that the set of constraints (31) are needed to linearise the objective function in the three models, and the set of equations that uses the binary expansion approach for pipes (35) and pumps (37), are needed for the BEA model.

4. Computational Experiments

The three alternative models defined in Section 3 were tested on three different and realistic high-altitude WSSs using the Gurobi 10 solver [58] via Julia [59]; the experiments were done using long and steep networks that send desalinated water from the sea level up to the mountains (more than 3000 m above sea level). For this work, it is assumed that the water production at the desalination plant and the mine site's water demand are constant. Table 1 summarises the main characteristics of the WSSs tested.

Table 1. WSS characteristics. Note that the "Tank" category includes the reservoirs, and the "Pipe Length" is the sum of all the WSS pipes.

WSS Size	Pump	Tank	Reservoir	Mine	Water Demand	Elevation	Pipe Length
Small (S)	5	5	1	1	1.50 m^3/s	3100 m	153 km
Medium (M)	6	4	6	6	1.00 m^3/s	3736 m	424 km
Large (L)	14	12	3	3	4.05 m^3/s	2400 m	669 km

In Figure 4, there is an example of a real WSS that pumps up desalinated water to a mine located at 3100 m.a.s.l. in the Chilean Atacama desert [2]. This water network corresponds to the Small WSS tested, and it has one reverse osmosis desalination plant and five interconnected pumping stations, combined with a water pump and tank, one reservoir, and one mine, which has a water demand. The data for the nodes and arcs can be seen in Tables 2 and 3.

Table 2. Data of the nodes of the Small WSS.

Node	Altitude [m]	Type of Node	Area Tank [m^2]	Height Tank [m]	Initial/Final Storage	Demand [m^3/s]
1	30	RO	-	-	-	−2.0
2	30	Tank	800	10	50%	-
3	1100	Junction	-	-	-	-
4	1100	Tank	800	10	50%	-
5	1600	Junction	-	-	-	-
6	1600	Tank	800	10	50%	-
7	2100	Junction	-	-	-	-
8	2100	Tank	800	10	50%	-
9	2600	Junction	-	-	-	-
10	2600	Tank	800	10	50%	-
11	3100	Junction	-	-	-	-
12	3100	Reservoir	1000	16	90%	-
13	3100	Mine	-	-	-	1.5

Table 3. Data of the arcs of the Small WSS.

Node from	Node to	Type of Arc	Length [m]
1	2	Pipe	1
2	3	Pump	30
3	4	Pipe	6300
4	5	Pump	-
5	6	Pipe	85,000
6	7	Pump	-
7	8	Pipe	21,800
8	9	Pump	-
9	10	Pipe	22,500
10	11	Pump	-
11	12	Pipe	17,400
12	13	Pipe	1

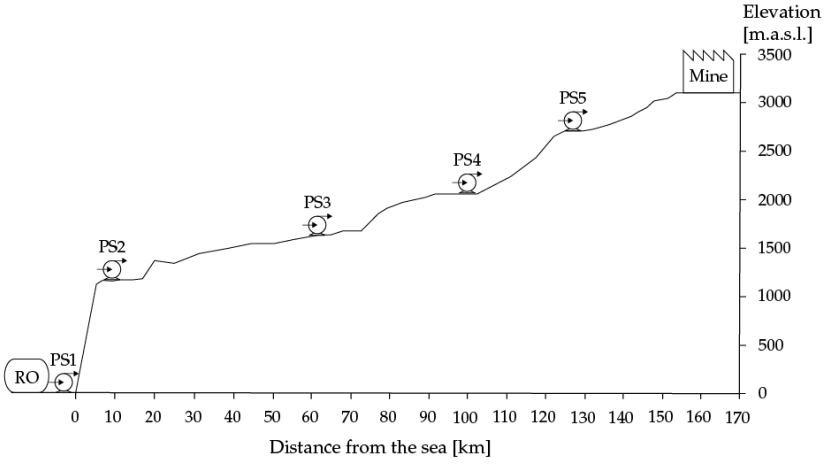

Figure 4. Conceptual representation of the water supply system topography for Radomiro Tomic (RT) Copper Chilean mine operation. This WSS corresponds to the small-sized water network with one reverse osmosis desalination plant, five pumping stations, and one mine.

Figure 2 shows a medium-size WSS proposed by [50] to supply water to six mining sites. It has ten pumping stations and six reservoirs. The data for the nodes and arcs can be seen in Tables 4 and 5.

Table 4. Data of the nodes of the Large WSS.

Node	Altitude [m]	Type of Node	Area Tank [m^2]	Height Tank [m]	Initial/Final Storage	Demand [m^3/s]
{1,2}	0	RO, Tank	800	10	50%	−1.50
{3,4}	660	Junction, Tank	800	10	50%	-
{5,6}	1220	Junction, Tank	800	10	50%	-
{7,8,34}	1260	Junction, Reservoir, Mine	1000	16	90%	0.90
{9,10}	1705	Junction, Tank	800	10	50%	-
{11,12,13,24}	2400	Junction, Reservoir, Mine, Junction	1000	16	90%	1.35
{14,15}	0	RO, Tank	800	10	50%	−2.00
{16,17}	700	Junction, Tank	800	10	50%	-
{18,19}	1395	Junction, Tank	800	10	50%	-
{20,21}	1450	Junction, Tank	800	10	50%	-
{22,23,33}	2045	Junction, Tank, Junction	800	10	50%	-
{25,26}	0	RO, Tank	800	10	50%	−1.00
{27,28}	545	Junction, Tank	800	10	50%	-
{29,30}	1045	Junction, Tank	800	10	50%	-
{31,32,35}	1630	Junction, Reservoir, Mine	1000	16	90%	1.80

Table 5. Data of the arcs of the Large WSS.

Node from	Node to	Type of Arc	Length [m]	Node from	Node to	Type of Arc	Length [m]
1	2	Pipe	1	20	21	Pipe	50,000
2	3	Pump	-	21	22	Pump	-
3	4	Pipe	8340	22	23	Pipe	52,600
4	5	Pump	-	23	24	Pump	-
5	6	Pipe	14,500	25	26	Pipe	1
6	7	Pump	-	26	27	Pump	-
7	8	Pipe	49,500	27	28	Pipe	11,500
8	9	Pump	-	28	29	Pump	-
9	10	Pipe	53,400	29	30	Pipe	60,400
10	11	Pump	-	30	31	Pump	-
11	12	Pipe	44,000	31	32	Pipe	73,200
12	13	Pipe	1	32	33	Pump	-
14	15	Pipe	1	8	34	Pipe	1
15	16	Pump	-	9	21	Pipe	42,900
16	17	Pipe	30,500	22	32	Pipe	49,700
17	18	Pump	-	33	23	Pipe	44,000
18	19	Pipe	37,500	32	35	Pipe	1
19	20	Pump	-	24	12	Pipe	43,500

Finally, a bigger water network is considered using data from [50], with fourteen pumping stations, one reservoir, and one mine, as seen in Figure 5. The data for the Large WSS can be found in the Tables 6 and 7.

Table 6. Data of the nodes of Medium WSS.

Node	Altitude [m]	Type of Node	Area Tank [m^2]	Height Tank [m]	Initial/Final Storage	Demand [m^3/s]
{1,2}	0	RO, Tank	800	10	50%	−1.50
{3,4}	866	Junction, Tank	800	10	50%	-
{5,6,22}	1461	Junction, Reservoir, Mine	1000	16	90%	0.10

Table 6. *Cont.*

Node	Altitude [m]	Type of Node	Area Tank [m^2]	Height Tank [m]	Initial/Final Storage	Demand [m^3/s]
{7,8}	2126	Junction, Tank	800	10	50%	-
{9,10}	3007	Junction, Tank	800	10	50%	-
{11,12,13}	3730	Junction, Reservoir, Mine	1000	16	90%	0.15
{14,15}	3342	Reservoir, Mine	1000	16	90%	0.20
{16,23}	1703	Reservoir, Mine	1000	16	90%	0.15
{17,20,21}	2424	Junction, Reservoir, Mine	1000	16	90%	0.30
{18,19}	2335	Reservoir, Mine	1000	16	90%	0.10

Table 7. Data of the arcs of the Medium WSS.

Node from	Node to	Type of Arc	Length [m]	Node from	Node to	Type of Arc	Length [m]
1	2	Pipe	1	12	13	Pipe	1
2	3	Pump	-	11	14	Pipe	31,100
3	4	Pipe	3410	14	15	Pipe	1
4	5	Pump	-	7	16	Pipe	36,400
5	6	Pipe	57,900	16	17	Pump	-
6	7	Pump	-	17	18	Pipe	66,300
7	8	Pipe	46,900	18	19	Pipe	1
8	9	Pump	-	17	20	Pipe	41,500
9	10	Pipe	84,300	20	21	Pipe	1
10	11	Pump	-	6	22	Pipe	1
11	12	Pipe	31,100	16	23	Pipe	1

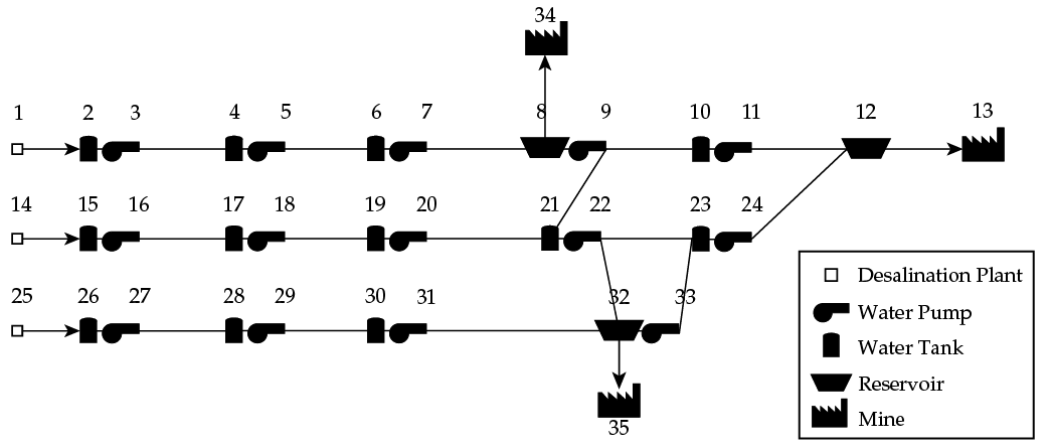

Figure 5. Diagram of the Large WSS used in this study. The numbers represent the nodes.

The values of other parameters for the model were obtained from [2]: water density, $\rho = 1000$ {Kg/m^3, pump efficiency, $\nu = 80\%$, pipe maximum speed, $v_{max} = 2.5$ m/s, pipe diameter, $D = 1$ m, Darcy friction factor, $f = 0.01$, pump linear parameter, $\beta_{i,j,t} = 1/q_{i,j,t}^{max}$, using the technique in [48], and the minimum water tank level percentage, $\gamma_i^{min} = 80\%$, which depends on the industry; in this case, $\gamma_{i,COD}^{min} = 95\%$ from CODELCO, a copper mining company. Finally, the electricity prices were obtained from the Chilean national electrical operator.

For example, Figure 6 shows the expected normalised results for the water pump scheduling problem in a WSS with one pump. The operator of WSSs desires to know every hour which water pumps turn on or off, what the level of the water tanks is, how much energy is being used, and what the operation cost is. Additionally, if water demands change over time, the operator wants to know if hourly or daily water demand is being met; otherwise, the model information would have to be updated, and other policies would

have to be taken in the following period. Note that the maximum number of time slots when the water pumps can be active is 125 for the Small WSS, 150 for the Medium WSS, and 325 for the Large WSS. It is 325 instead of 350 because there is one water pump that has never been activated due to the network design.

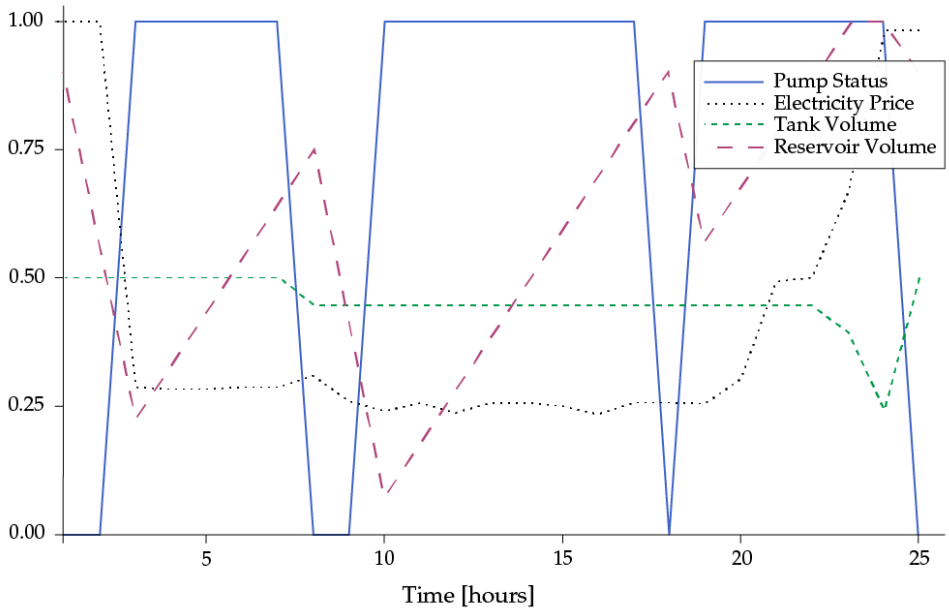

Figure 6. Example of a WSS with one pump and its expected results for the water pump scheduling problem. The volume of the water tanks and reservoirs, the electricity price, and the water pump status values are normalised and displayed in the same plot to analyse its variation per hour.

The following subsection presents the different computational experiments analysed to understand the efficiency of the proposed method and the key parameters and variables of the water pump scheduling problem.

4.1. Choosing the Appropriate Cost of Maintenance C_s

As we explained in the section on the objective function, the pump switching can negatively affect the water system's maintenance cost, C_s, due to the changing load contributing to fatigue-related failures [45]. Following the recommendations of [20], which consists of trying different values of C_s for a given vector of electricity prices, C_t, when the maintenance cost is unknown.

We analysed the C_s value for the Small, Medium, and Large WSSs using different electricity prices. For this purpose, we utilised two prices: the variable price was taken from the Chilean Electricity Coordinator from a summer day in 2021 in the Radomiro Tomic Electric Bus, and the simple price is a simplified representation of the previous cost, with only two values, one for peak and one for non-peak hours. We chose the values of the simple price, such that the mean and variance were similar to the variable price, and it is a reasonable structure since some markets work in a high/low price scheme. In Figure 7 are shown the electricity prices for both the simple and the variable price.

Then, for each electricity price, we studied the impact of constraint (21) using a 90% minimum water level of the reservoir in each hour. We chose this value because it provides enough flexibility to the water pumps to have more time slots to be off, but it is high enough so that the demand node is secured with a safe level of water. In the following sections, we analyse the study case for the Small WSS using a 95% minimum water level because the mining company is highly conservative with the amount of water they need. Otherwise, in a water pump supply failure scenario, the cost of loss for their mining operation is extremely expensive.

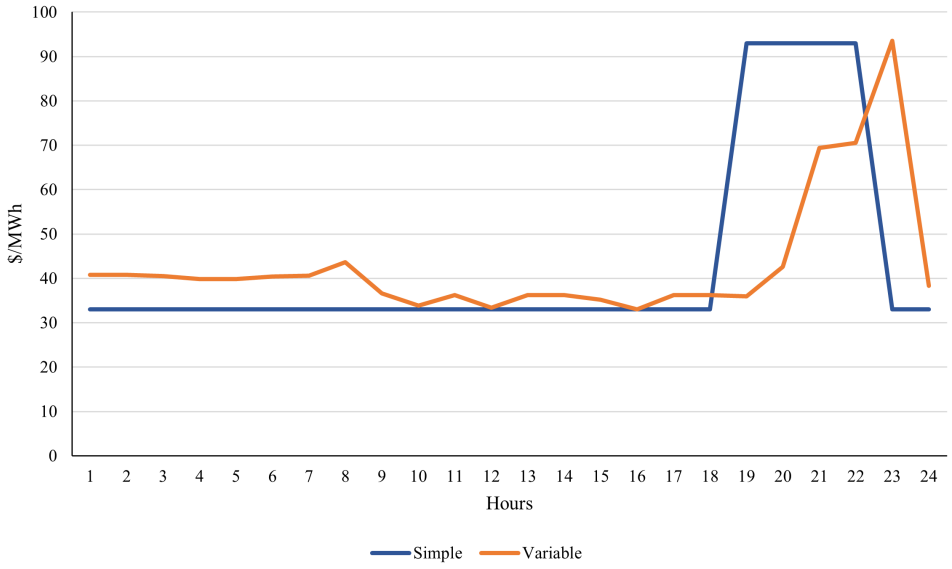

Figure 7. Hourly electricity prices in our case study. The variable price was taken from a summer day of 2021 in the Radomiro Tomic electric bar in the northern region of Chile. The simple price is a simplification of the variable, with only two values: one for the peak and the other for the non-peak hours.

For example, for the Small WSS, with a simple electricity price, as we can see in Figures 8 and 9, from $C_s = \$30$, the maintenance cost makes all the water pumps active; however, the same scenario occurs for the reservoir constrained case, with $C_s = \$20$. This result makes complete sense since the reservoir constraint increases the total cost, as it reduces the feasible region, and therefore the new global optimum can be excluded. Note that from those C_s values, the optimal value and the operational costs remain constant, even though the maintenance values increase. This is due to no switching being done; therefore, $B_{i,j,t} = 0$, which makes the maintenance costs zero in the optimal value. This pattern is repeated in any electricity price analysis.

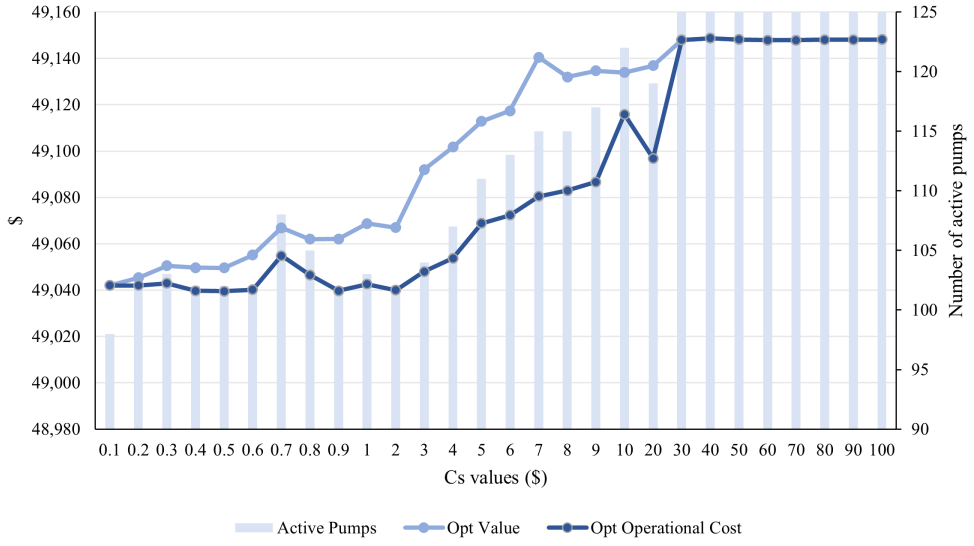

Figure 8. C_s values for the simple electricity price in the Small WSS. The total costs (opt. value), the operational costs, and the active water pumps are displayed. The model was solved using the SL model with a stop of a maximum of 20 s.

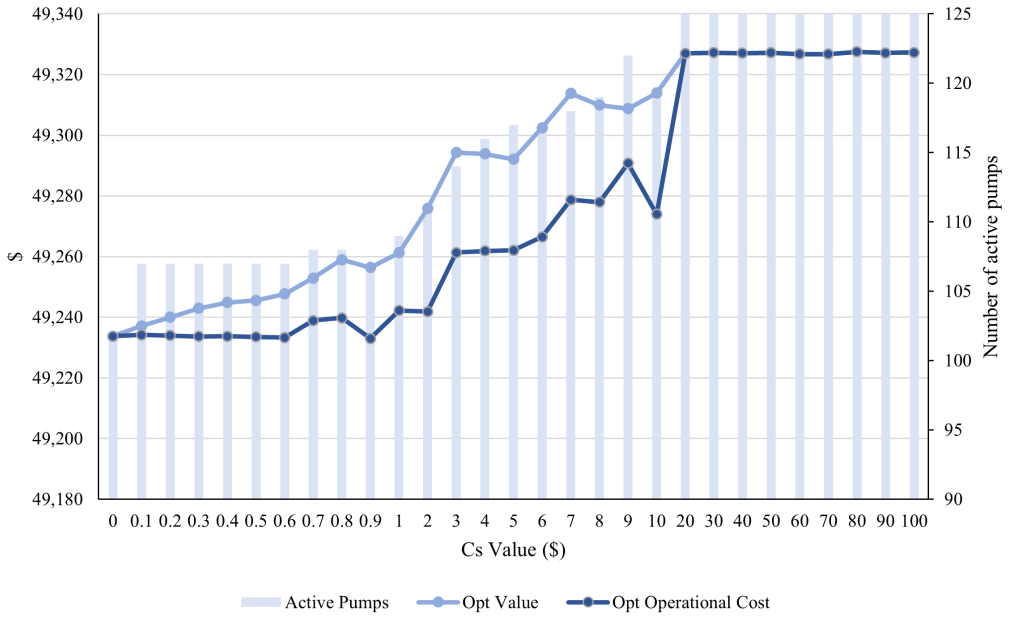

Figure 9. C_s values for the simple electricity price with the fixed reservoir constraint of 90% in the Small WSS. The total costs (opt. value), the operational costs, and the active water pumps are displayed. The model was solved using the SL model with a stop of a maximum of 20 s.

In order to select an appropriate C_s value, we would like to have at least 15% of flexibility in the number of active pumps, i.e., for the Small WSS, around 15–18 slots of inactive pumps in total in a 24 h horizon. This is achieved with $C_s = \$4$ for the unconstrained case and with $C_s = \$2$ for the constrained case.

A similar study was done with the variable electricity price. Since it has a slightly higher variance than the simple electricity price, it is expected that the C_s needs to be smaller to compensate for the total cost, as we can observe in Figures 10 and 11. For this case, the chosen value is $C_s = \$3$ for the unconstrained case and $C_s = \$1$.

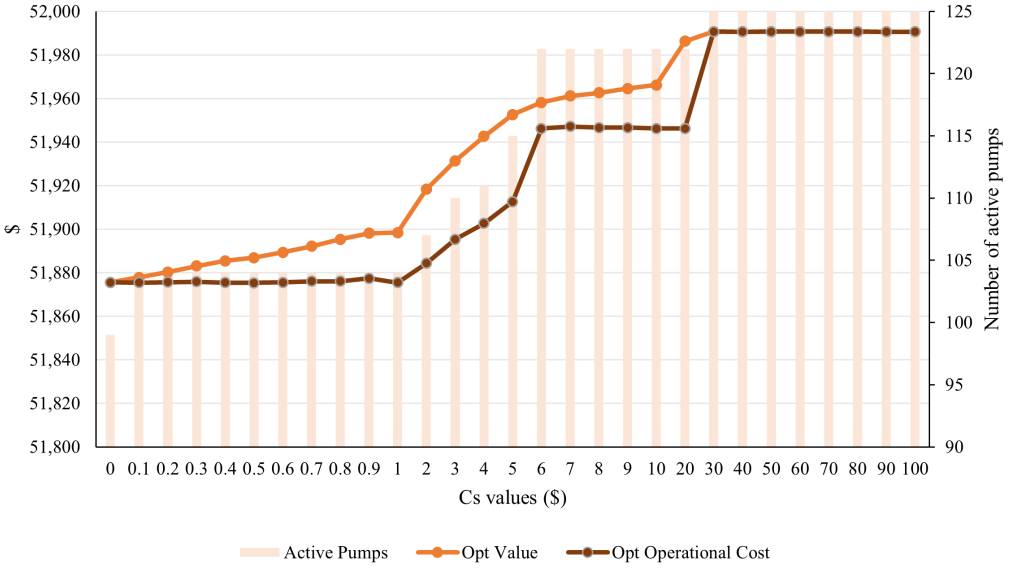

Figure 10. C_s values for the variable electricity price in the Small WSS. The total costs (opt. value), the operational costs, and the active water pumps are displayed. The model was solved using the SL model with a stop of a maximum of 20 s.

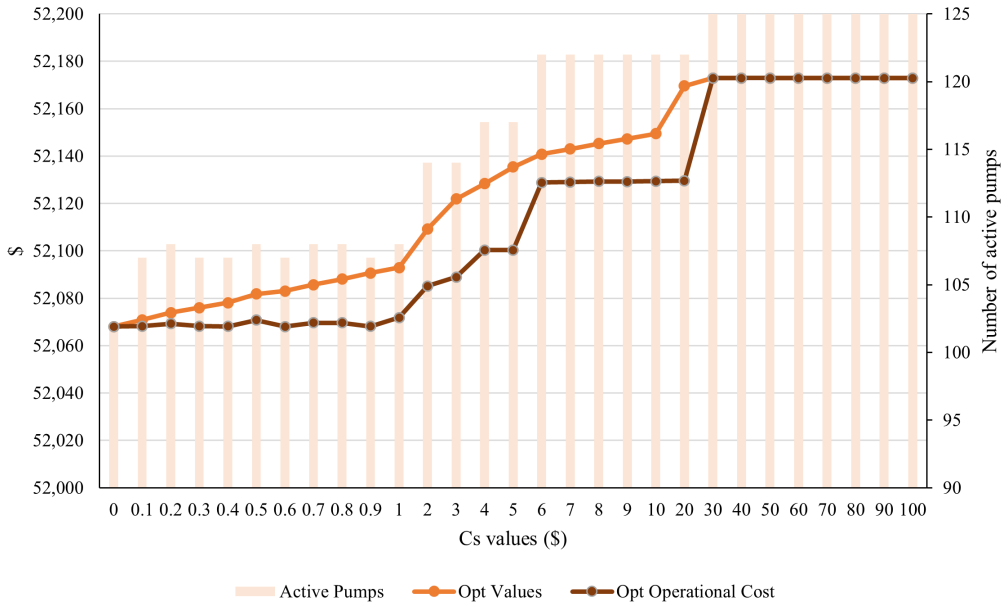

Figure 11. C_s values for the variable electricity with the fixed reservoir constraint of 90% in the Small WSS. The total costs (opt. value), the operational costs, and the active water pumps are displayed. The model was solved using the SL model with a stop of a maximum of 20 s.

4.2. Comparison of Running Times

In Table 8 are the significant results for the Small, Medium, and Large WSSs using the variable electricity price, not activating the reservoir constraint (21) and the MINLP approaches: fixed flow (FF), semi-linear (SL), and the MILP binary expansion approach (BEA). The optimality gap of the MINLP methods is 0% in most of the cases. We ran the model using a Windows 11 computer with 11th Gen Intel(R) CORE(TM) i7-1165G7 @2.80GHz. It is worth mentioning that solving the original model (24) and the FF model for more significant instances takes too long, so we had to set a 10 min time stop to the Gurobi solver in order to add those results to the table. Otherwise, it could have taken more than 7 h to complete. Also, for this work we consider that the SL model reaches the optimal value of this problem because the other approaches are either an upper bound (FF) or a binary approximation (BEA) of the original problem.

Table 8. Comparison of the three models using different WSS sizes using an 11th Gen Intel(R) CORE(TM) i7-1165G7 @2.80GHz.

Model	Size	Time	Obj. Value	Active Pumps	Power	Gurobi Gap
FF	S	4.67 s	$51,951	125	1388 MW	0.01%
SL	S	3.62 s	$51,931	110	1352 MW	0.01%
BEA (N = 3)	S	1.54 s	$51,894	118	1352 MW	0.49%
FF	M	10 min	$30,395	117	853 MW	0.01%
SL	**M**	**10 min**	**$30,449**	117	853 MW	**0.01%**
BEA (N = 4)	M	1.3 min	$30,360	117	852 MW	0.91%
BEA (N = 2)	**M**	**8.68 s**	**$30,382**	118	853 MW	**0.91%**
FF	L	10 min	$85,439	281	2242 MW	0.03%
SL	L	10 min	$85,540	279	2343 MW	0.03%
BEA (N = 4)	L	17.3 s	$85,462	275	2238 MW	0.89%
BEA (N = 2)	L	7.44 s	$85,527	281	2240 MW	0.89%

We performed different experiments using the binary expansion approach (N = 4 for M and L, and N = 3 for S) with Gurobi MILP, which reduces the computational time of the

original MINLP while keeping the Gurobi Gap within 0.9%. Also, the BEA model slightly reduces the optimal value because it is an approximation of the original problem.

The main difference is seen in the Medium and Large WSSs because they not only have more pumps and tanks, but the Medium is higher, and the Large has a bigger water demand, which makes them computationally intensive to solve due to the higher number of possible combinations. In the following sections, we explain this phenomenon in more detail.

It is worth mentioning that solving this problem with Ipopt, a free nonlinear solver, is not possible due to the mixed integer nature of this problem, which it does not support. Also, it only ensures global optimality for convex problems, and this is non-convex. Therefore, we decided to use the Gurobi solver to obtain global optimum results in a reasonable time.

We included the power required in a day because it is a good indicator of the solution's quality. As we can see in Table 8, the optimal power needed for each WSS tested was similar for the three models: 1352 MW for the Small, 853 MW for the Medium, and 2343 MW for the Large. Note that even though the Medium WSS is the highest one, its water demand is 1 m^3/s, compared with 1.5 m^3/s for the Small and 4.05 m^3/s for the Large. Therefore, the power needed was less than for the other cases.

In all the tested cases, the BEA model runs faster than the other models; furthermore, the goal of BEA is to obtain feasible solutions quicker with a reasonable gap because the water operator needs to make its decisions on a day-ahead basis.

4.3. Computational Impact of Network Altitude and Length

As we mentioned before, the model's most significant parameter is the highest node's altitude. This is because, by increasing its maximum altitude, the model takes longer to solve due to the increase in total combinations it has to compute. We computed experiments using the Medium WSS by dividing its altitude and total pipe length by ten and comparing the results. Table 9 shows the results for a medium-sized WSS using Model BEA (N = 4) and 0.5% Gurobi Gap.

Table 9. Comparison of different altitudes and pipe length using medium-size network.

Experiment	High (3736 m)	Low (373 m)
Long (424 Km)	**1.33 min**	10.93 s
Short (42 Km)	**1.73 min**	18.12 s

When the altitude of a WSS decreases, the model has fewer possible combinations to choose from because it can send less water to the following nodes in each period of time and still meet the water demand compared to the high-altitude scenario. This becomes even more computationally intensive when the pipe length is shorter because, since the distances are smaller, there are more possibilities to send water in each period of time. The same pattern can be seen in Table 8, since the Medium WSS is slower to compute because it is the highest of the three WSS tested.

Therefore, the altitude, meaning the maximum height difference between any two nodes in a water network, is the most relevant characteristic of the WSS operation because it augments the complexity of the model resolution. Hence, it becomes a relevant problem to be solved, especially in water networks that supply multimillion-dollar industries, which depend on those inflows.

4.4. Impact of the Number of Partitions in BEA

It is evident that the higher the number of partitions in the binary expansion approach, the closer the results will be to their actual value. However, when the N value increases, the computational time of the model increases (see Table 10). Therefore, choosing a reasonable value for N is crucial to have a good balance between the computational time and the optimal solution.

Table 10. Comparison of different N partitions in BEA for the Small WSS. We used a fixed MIPGap of 0.9%.

N	Time	Obj. Value	Active Pumps	Power	Gurobi Gap	SL Gap
1	0.50 s	\$51,949	115	1352 MW	0.22%	0.03%
2	0.99 s	\$51,915	114	1352 MW	0.39%	−0.03%
3	**1.54 s**	**\$51,894**	**118**	**1352 MW**	**0.49%**	**−0.07%**
4	**3.75 s**	**\$51,876**	**117**	**1351 MW**	**0.65%**	**−0.11%**
5	**5.57 s**	**\$51,867**	**119**	**1351 MW**	**0.70%**	**−0.12%**
6	14.06 s	\$51,858	116	1351 MW	0.62%	−0.14%
7	20.07 s	\$51,854	112	1350 MW	0.75%	−0.15%
8	20.09 s	\$51,852	117	1351 MW	0.82%	−0.15%
9	27.83 s	\$51,851	118	1351 MW	0.88%	−0.16%
10	33.52 s	\$51,850	111	1350 MW	0.89%	−0.16%
20	79.68 s	\$51,853	112	1350 MW	0.94%	−0.15%
30	10 min	\$51,853	115	1350 MW	1.20%	−0.15%
40	10 min	\$51,847	117	1350 MW	1.07%	−0.16%
50	10 min	\$51,851	117	1350 MW	1.16%	−0.15%

To select the right *N* value, we used two Gaps to analyse and compare its performance: the Gurobi Gap and the SL Gap. By Gurobi Gap, we mean the MILP gap given by Gurobi, which uses the objective bounds: the incumbent and the best bound found so far. On the other hand, the SL Gap is the relative error between the optimal objective value of the BEA method in the n-th value and the optimal value of the SL model, assuming that that is the global optimum of the problem.

From these results, for the small-sized WSS, from N = 6 partitions, the Gurobi Gap and SL Gap do not improve much, while the computational time increases rapidly. It is interesting to mention that when the N value is too high, for example, N = 200, the computer cannot process the model, so it stops after a few seconds with a bad solution (around 30% Gurobi Gap). Note that we set a time stop in 600 s for the bigger *N* values; otherwise, the problem would take several minutes or hours to reach the 1% Gurobi Gap. It is relevant to mention that if the Gurobi Gap is too high or the time limit is too low, most of the time, the number of active pumps will be the maximum value, i.e., for the Small WSS it is 125; essentially, all the pumps are on in all the time periods.

Therefore, depending on the size of the WSS, the recommended number of partitions for the BEA model is between 3 and 5. This allows the model to be solved rapidly with reasonably small Gurobi and SL optimality gaps and a more accurate number of active pumps.

4.5. CODELCO Radomiro Tomic WSS Case Study

The optimal outcome in an optimisation model varies depending on the input data provided, and in this case the model should demonstrate sensitivity to the seasons of the year in regions where there is a clear differentiation in temperature, which consequently affects electricity prices. This section analyses the impact of the seasons of the year, the minimum reservoir level, the CODELCO energy policy, and the increase in water demand. We use as a case study for this work the Small WSS called "Aguas Horizonte," which corresponds to the supply water network for the "Radomiro Tomic Mine" of the company CODELCO in the northern region of Chile.

The results studied from this section onwards include changes in the water tanks and reservoir capacities, the initial/final storage for the reservoir, and the water demand at the mine site of the Small WSS, obtained from the "Aguas Horizonte" environmental analysis report [60] to ensure maximum realism for the energy and economic analyses. The new data for the nodes of the CODELCO Small WSS are displayed in Table 11.

Table 11. Data of the nodes of the Small WSS for the study case of Radomiro Tomic Mine WSS.

Node	Altitude [m]	Type of Node	Area Tank [m^2]	Height Tank [m]	Initial/Final Storage	Demand [m^3/s]
1	30	RO	-	-	-	−2.0
2	30	Tank	1136	8.82	50%	-
3	1100	Junction	-	-	-	-
4	1100	Tank	314	11.3	50%	-
5	1600	Junction	-	-	-	-
6	1600	Tank	314	11.3	50%	-
7	2100	Junction	-	-	-	-
8	2100	Tank	314	11.3	50%	-
9	2600	Junction	-	-	-	-
10	2600	Tank	314	11.3	50%	-
11	3100	Junction	-	-	-	-
12	3100	Reservoir	15,625	16	95%	-
13	3100	Mine	-	-	-	1.5

4.5.1. Impact of Seasonal Electricity Prices

We selected random days from autumn, winter, spring, and summer for this analysis. The electricity prices for these days are depicted in Figure 12, corresponding to the following dates: 31 March 2024 for autumn, 22 July 2023 for winter, 20 October 2023 for spring, and 19 January 2024 for summer.

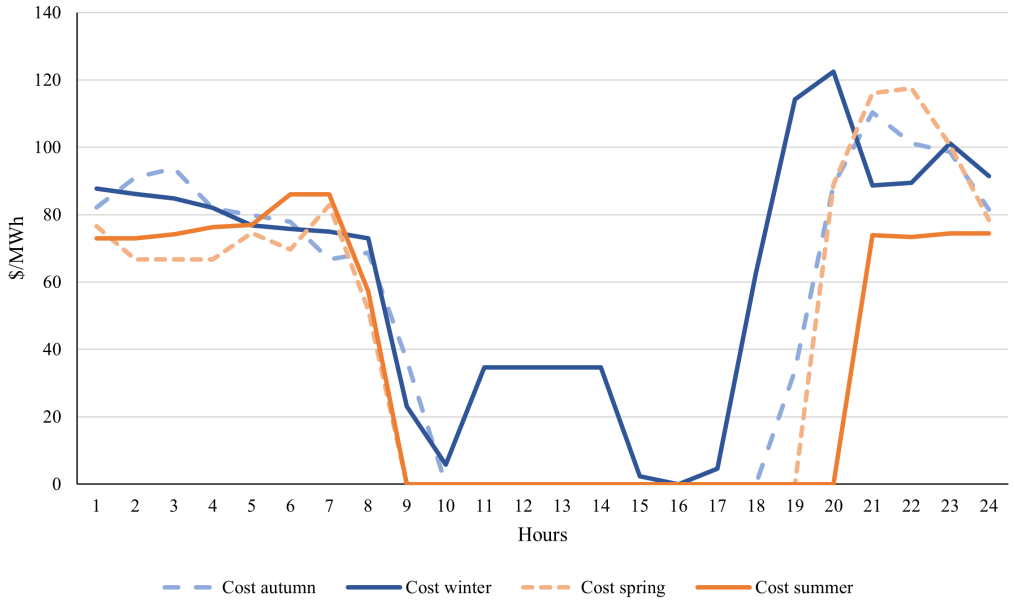

Figure 12. Hourly electricity prices per season for the Radomiro Tomic electric bar in the northern region of Chile. Data taken from the Chilean Electricity Operator. The days per season correspond to the following days: 31 March 2024 for autumn, 22 July 2023 for winter, 20 October 2023 for spring, and 19 January 2024 for summer.

As anticipated, the warmer months exhibit lower prices compared to the colder months. Moreover, during wintertime, there are fewer hours with USD 0 MWh, possibly due to reduced solar generation. However, because winter experiences higher minimum prices, its dispersion is lower, as illustrated in Figure 13.

Summertime records the lowest mean and median of the year, averaging around USD 30 MWh, in contrast to the USD 65 MWh observed during winter. Autumn and spring demonstrate similar behaviour, with a mean of approximately USD 50 MWh. Additionally, the median for summer is lower than its mean, indicating that there are more values below the mean, including USD 0 MWh, while the higher values contribute to its average.

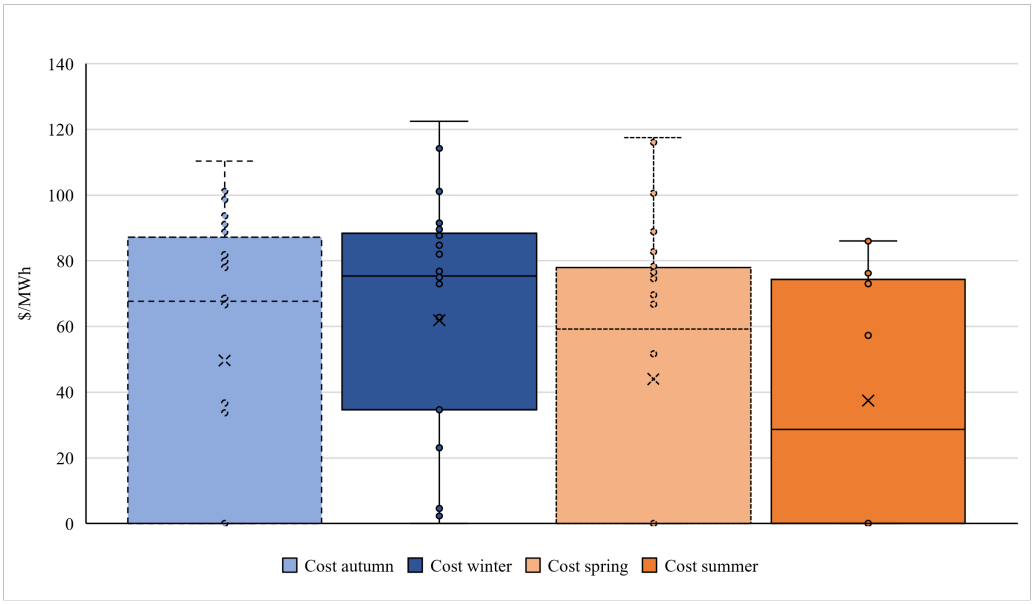

Figure 13. Electricity prices dispersion per season for the Radomiro Tomic Electric Bar.

Lastly, for each season, it was necessary to select an appropriate value for the maintenance cost, C_S, to switch the water pumps between periods. Following the same methodology as in the preceding sections, we determined that for the Small WSS, C_s = \$3 for each season.

Using the seasonal electricity prices, we examined their impact on the water pump scheduling problem. In Figure 14, we can observe that the optimal objective value follows the same pattern as the mean and median of the electricity prices; namely, winter is the most expensive, followed by autumn, spring, and finally summer. This trend persists when implementing policies such as incorporating the minimum water level in the reservoir for each hourly constraint (21) and restricting the number of active pumps during certain hours of the day, as elaborated in subsequent sections.

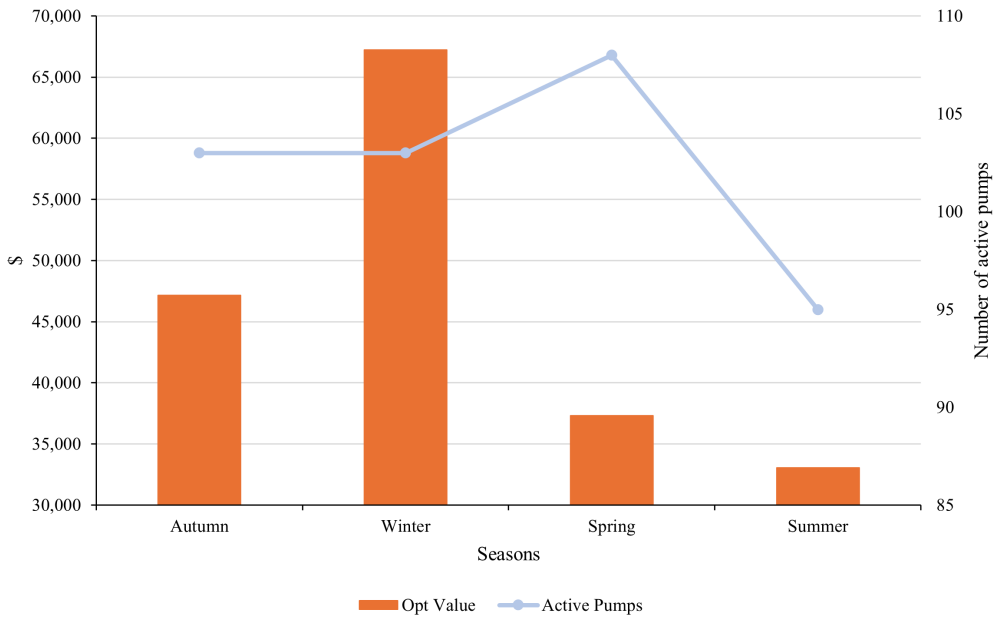

Figure 14. Objective values for the Small WSS with the new water tanks and reservoirs values, using the electricity prices per season and the model BEA (N = 3, Cs = USD 3, Gurobi Gap = 0.5%) for the Radomiro Tomic Electric Bar.

Moreover, from Figure 14, it is noteworthy that, during spring, the number of active pumps increases, presumably because the problem aims to activate them during hours when electricity costs are USD 0 MWh.

4.5.2. Security and Energy Policies

For this case study, we examined two policies concerning the utilisation of reservoirs and water pumps throughout the day: firstly, the implementation of a minimum water level constraint for reservoirs for each hour (Res), as described in constraint (21), and secondly, the imposition of a maximum limit on the number of active pumps within a specified time period (Pol). Detailed explanations of each policy are provided in the subsequent sections.

1. Impact of minimum water tank and reservoir levels (Res)

As previously discussed, the degree of flexibility concerning the minimum water tank and reservoir parameters may vary depending on the industry. This variation is determined by the company's opportunity cost in reducing its minimum water level to mitigate energy expenses and the potential risk of inadequate water supply should all systems fail, leading to a multimillion-dollar loss for each minute its operation stops.

Therefore, we use the constraint (21):

$$h_{i,t} \geq Z_i + \bar{h}_i \gamma_i^{min}, \forall i \in R, \ \forall t \in T,$$

and we analysed two cases for the γ_i^{min} parameter: 90% and 95%. For the case of CODELCO, they need a 95%; however, we wanted to study how much they can save if they reduce to 90% the minimum level of water in their reservoirs.

2. Cost Savings Relative to Current Policy (Pol)

Some industries manually optimise their processes, adhering to specific principles or rules based on their experience. However, such policies often lead to local optima. The energy policy under scrutiny in this section, pertaining to the CODELCO WSS, involves the cessation of water pump operations between 6 p.m. and 10 p.m. Initially, this may seem reasonable, considering that electricity demand typically peaks during the evening; nevertheless, the optimal results show otherwise.

For our analysis, we selected four days from each season of the year, using data from the Radomiro Tomic electric bus, as explained in the preceding section. We then compared this data with the company's energy policy. However, upon running the model with the company's energy policy, the problem results proved infeasible. Consequently, we opted to introduce the following constraint to the model, limiting the number of active pumps, denoted by r, during the 6 p.m. to 10 p.m. timeframe:

$$\sum_{t=18}^{22} x_{i,j,t} \leq r \qquad \forall (i,j) \in Pu, \tag{41}$$

First, for the minimum reservoir level $\gamma_i^{min} = 90\%$, the minimum number of active pumps that made the problem feasible was $r = 3$; however, when we increase γ_i^{min} to 95%, r becomes 4.

4.5.3. Comparison of Policies

Before analysing all the possible policy combinations in detail, Figure 15 shows us an insight into the most relevant policies for the water scheduling problem for the Radomiro Tomic WSS.

The policy combinations with the highest optimal values are the ones that use the CODELCO energy policy (Pol), especially in the warmer months, as we can see in Figure 16 compared with Figures 14 and 17. For the summertime, the cost without (Pol) policy goes from around USD 33,000 to USD 47,000 when the policy is applied. The same occurs in spring, going from around USD 37,000 to USD 50,000. Winter is the only season that

remains almost the same when the policy is applied, and this is because the electricity prices throughout the day are higher than in other seasons; therefore, the savings are minor when turning off almost all the water pumps between 6 p.m. and 10 p.m.

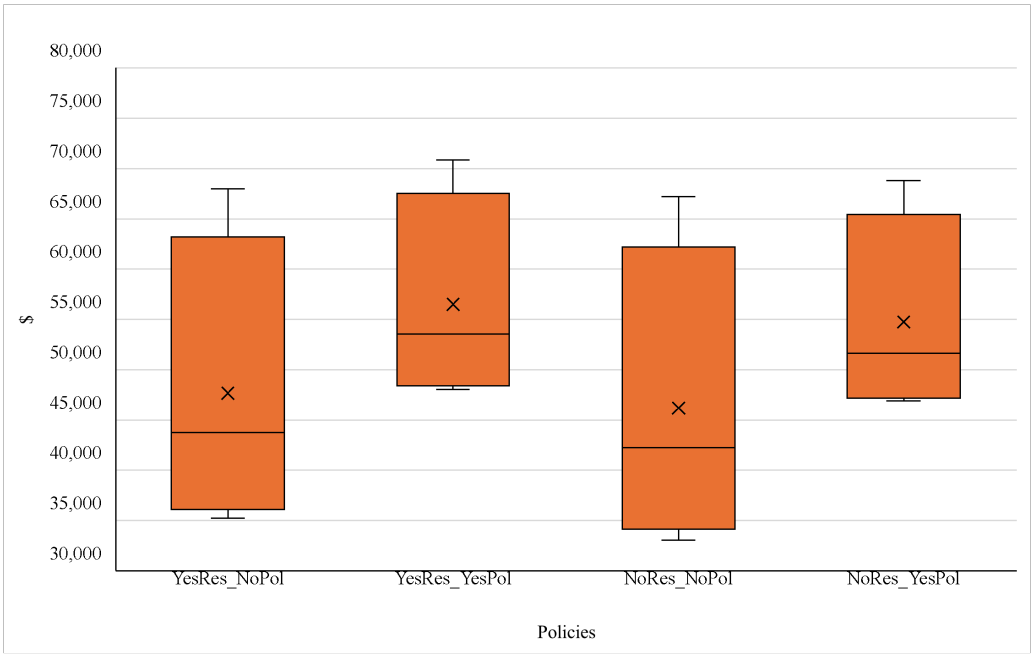

Figure 15. Objective values dispersion for the different policy combinations for the Small WSS using the electricity prices per season, different reservoir levels, and the CODELCO energy policy. Solved with BEA (N = 3, Cs = USD 3, Gurobi Gap = 0.5%) for the Radomiro Tomic Electric Bar.

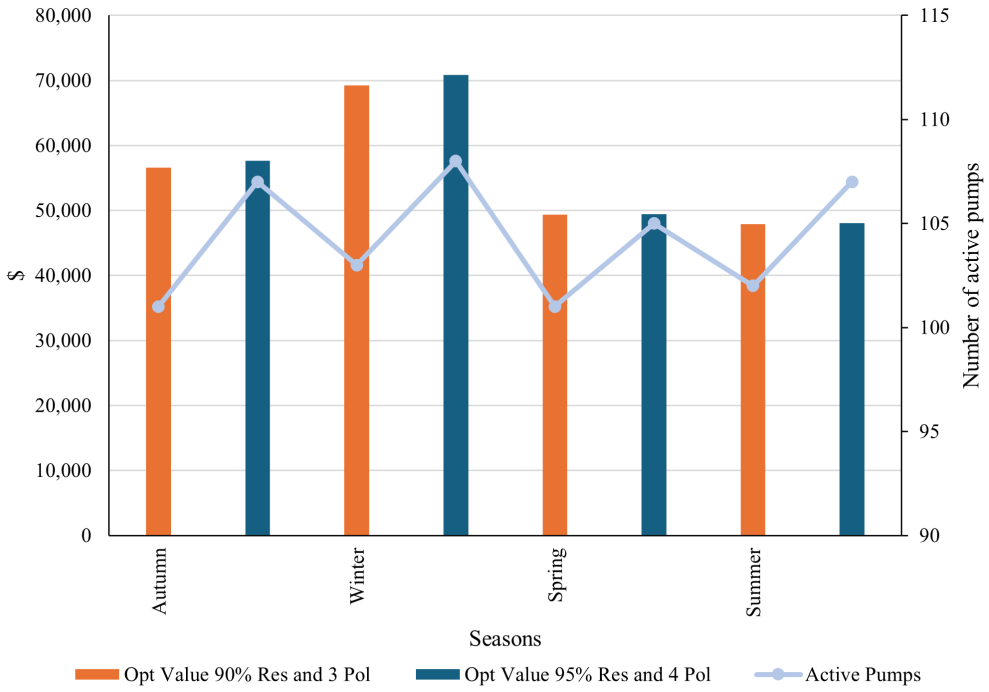

Figure 16. Optimal objective values for the Small WSS using the electricity prices per season, the different minimum levels in reservoirs, and the CODELCO energy policy. Solved with BEA (N = 3, Cs = USD 3, Gurobi Gap = 0.5%) for the Radomiro Tomic Electric Bar.

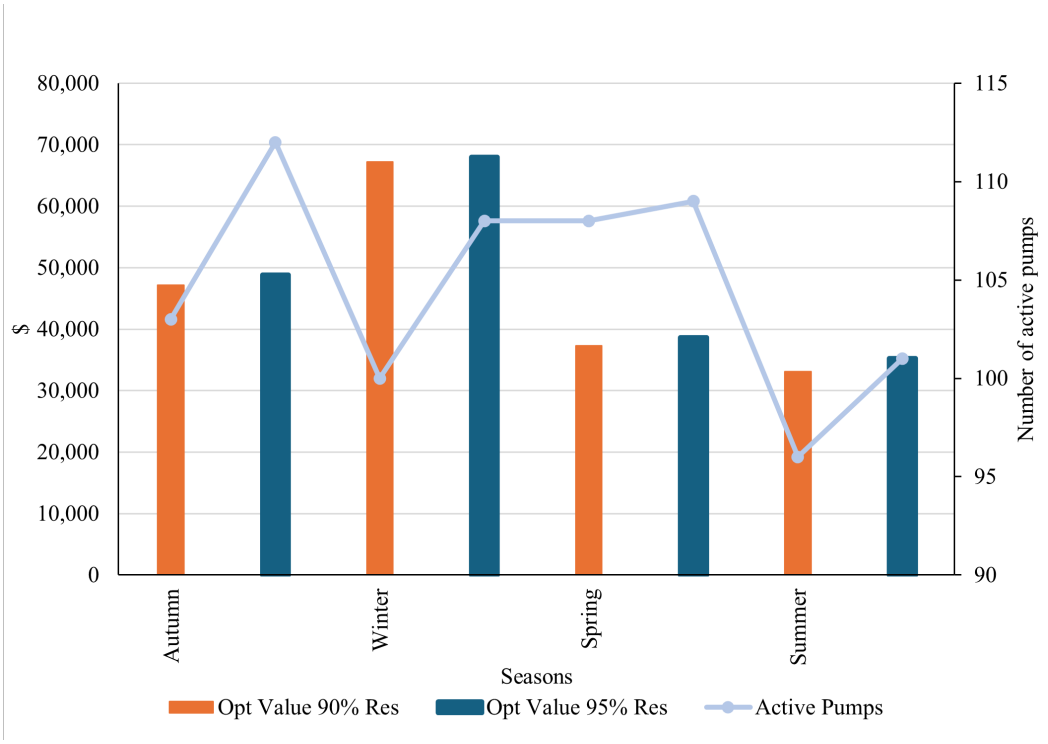

Figure 17. Objective values for the Small WSS using the electricity prices per season, different reservoirs levels. Solved with BEA (N = 3, Cs = USD 3, Gurobi Gap = 0.5%) for the Radomiro Tomic Electric Bar.

Also, we can see a small difference in the objective value when changing the minimum reservoir level from 90% to 95%, as CODELCO mining company requires: with the 90% level, the optimal objective value is smaller than with a 95% level. This occurs both whether the CODELCO energy policy (Pol) is applied or not, as we can see in Figures 16 and 17. The water pumps are activated less in the 90% case compared with the 95%, which gives more space to provide flexibility and ancillary services to the electrical grid as future work.

4.5.4. Impact of Higher Water Demand

One of the concerns the water consumer may have regarding the water operation and supply is how much pumping costs would increase or decrease if the water demand varies. To study this, we solved the Small WSS of CODELCO (Radomiro Tomic Mine) using BEA (N = 3, C_s = 3, Gurobi Gap = 0.5%) with no policies for each season and varied the mine water demand over a discretised range from 0.19 m^3/s to 1.96 m^3/s, which is the maximum water flow allowed by the water pipes.

The results are shown in Figure 18, confirming the anticipated trend: greater water demand correlates with a higher optimal objective function. Specifically, augmenting the original water demand of 1.5 m^3/s by an additional 0.46 m^3/s results in a roughly 70% rise in costs across all seasons. Additionally, the seasonal patterns persist, with warmer days associated with lower costs.

It is noteworthy that achieving a comparable cost to that of winter requires a 0.5 m^3/s increase in water flow during summer. In essence, while transporting approximately 1.6 m^3/s at USD 40,000 in summer achieves the same cost efficiency as in winter; only 1.1 m^3/s can be transported during the colder months.

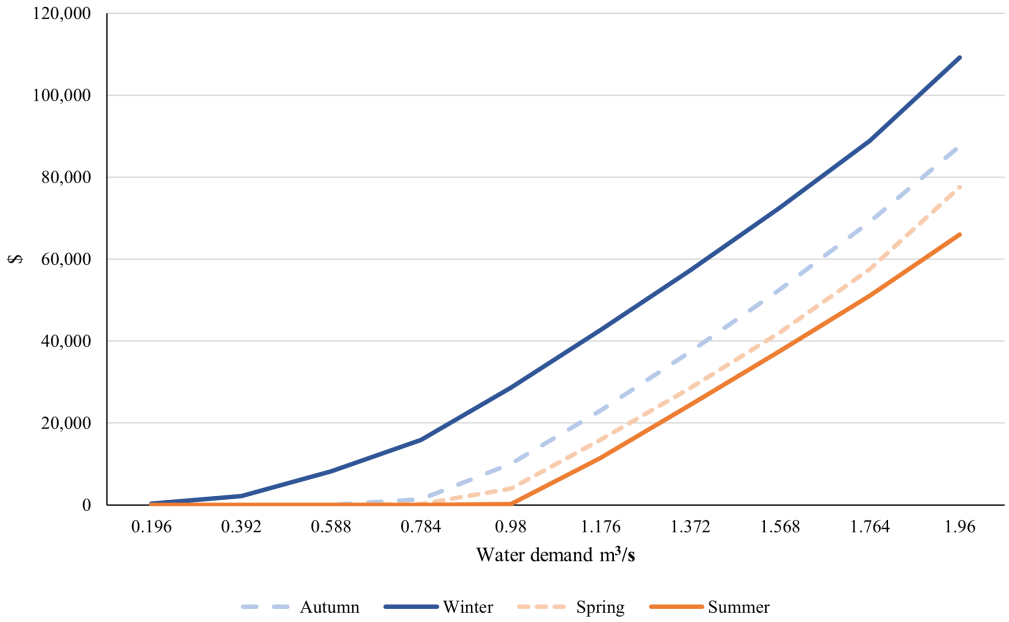

Figure 18. Objective values for the Small WSS using the electricity prices per season, varying the water demand from 0.19 m^3/s to 1.96 m^3/s. Solved with BEA (N = 3, Cs = USD 3, Gurobi Gap = 0.5%) for the Radomiro Tomic Electric Bar.

4.6. Computational Performance for Checking Optimality

An alternative way to compare the computational efficiency of different models is to investigate how quickly each model proves optimality. There are two ways of doing this: using the optimal solution and the optimal value to test the model.

The first way of doing this is by evaluating the model's speed when the optimal solution is given as the initial point. The first row of Table 12 in each block represents the model without using this initial point. The binary expansion approach is set to stop with a 0.5% Gurobi Gap to obtain the optimal solution. Then, that optimal solution is given as a starting point for the solver, and it always returns the new optimal solution with a 0% Gurobi Gap. In this case, the BEA with N = 3 model verifies the optimal solution in less than 2 s, whereas the MINLP problem using the Gurobi MINLP solver takes almost double that time. As expected, the higher the N value is, the longer it takes to solve.

Table 12. Setting as initial point the optimal solution with gap 0% to each model in the Small WSS.

Model	Initial Point	Time	Obj. Value
SL	**-**	**3.63 s**	**51,931**
SL	yes	1.66 s	51,931
BEA, N = 3	-	**1.54 s**	**51,894**
BEA, N = 3	yes	1.3 s	51,894
BEA, N = 8	**-**	83.22 s	51,844
BEA, N = 8	yes	66.55 s	51,844

The second way to verify if the restrictive approach is reaching optimality is by adding a constraint that is a lower bound for the optimal value. Like in the first optimality check, the second time the model is run the Gurobi Gap is 0%. In this approach, the BEA model is faster in realising that the optimal value is the same as the given constraint (see Table 13).

Table 13. Setting the optimal value constraint with gap 0% to each model in the Small WSS.

Model	Optimal Value	Time	Obj. Value
SL	-	**3.63 s**	**51,931**
SL	yes	11.15 s	51,931
BEA, N = 3	-	**1.54 s**	**51,894**
BEA, N = 3	yes	0.29 s	51,894

These results show us again, in computational terms, that the binary expansion approach is more efficient than the original formulation because it takes less time to verify that it is the optimal solution.

In summary, the BEA technique allows us to solve the optimal operation of a water network in a reasonable computational time with a small gap compared with other solvers. The latter is relevant because the water network operator needs to have a solution on a day-ahead basis. Also, the BEA approximation does not need to take a large number of partitions to obtain a good result. Henceforth, our recommendation is to use between three and five partitions, depending on the size of the water network.

5. Conclusions and Future Research

In this paper, a new application of the binary expansion approach was applied to the pump scheduling problem to linearise the optimisation model. The problem aims to optimise energy costs in large-scale, multi-tank, and high-altitude WSSs. The method was tested with a real-life WSS from the Radomiro Tomic Mine in Chile. The results obtained by using this approach were compared with other approximating techniques. The critical findings obtained are as follows:

1. In most cases, the binary expansion approach performs better than the MINLP Gurobi solver. The computational efficiency of the approach gives the chance to use it for hours or for day-ahead operation, such as in many types of electrical demand flexibility models in large WSSs.
2. The **altitude of a water network** is the parameter with the greatest impact on the solution time; that is, the higher the WSS, the slower the model will run due to the higher number of combinations the solver needs to verify. Also, the total length of the pipes is only relevant when the WSS altitude is high.
3. The **recommended number of partitions** in the binary expansion approach is between **three and five**, depending on the WSS characteristics. Using more than ten partitions is not suggested because the computational times increase rapidly, and the gap almost does not change.
4. The **influence of temperature** across various months significantly affects the overall expenses of WSS operations: the warmer the month, the cheaper the electrical tariffs become, leading to reduced operational costs as well.
5. The operational strategy of turning off the water pumps during a time period from 6 p.m. to 10 p.m. (Pol) amplifies expenses during warmer days by inhibiting pump usage during hours of lower electricity rates.
6. The operational strategy of having a minimum level of water in reservoirs of 90% or 95% yields minimal changes in costs; however, maintaining a lower level decreases the number of active pumps throughout the day, which allows a space to provide flexibility to the electrical grid in future endeavours.

Finally, the binary expansion approach can be used to further extensions of the problem, such as the WSS design problem, WSS capacity expansion planning problem, and demand response problem applied to WSS. In particular, we are analysing the use of WSSs as flexible sources for the power network by modifying the water pump scheduling problem to provide ancillary services to the power network while optimising the costs and revenues of the water network operator.

Author Contributions: D.C., conceptualisation, methodology, software, validation, formal analysis, investigation, resources, data curation, writing—original draft preparation, writing—review and editing, visualisation, project administration, funding acquisition; Á.L., conceptualisation, validation, writing—review and editing, supervision; M.F.A., conceptualisation, validation, writing—review and editing, supervision. All authors have read and agreed to the published version of the manuscript.

Funding: The authors thank ANID for their funding through the "DOCTORADO NACIONAL 21211385" scholarship and "FONDECYT-1211378" project, and CODELCO for their funding through the "Beneficio Piensa Minería".

Data Availability Statement: All data are available within the article.

Conflicts of Interest: The authors declare no conflicts of interest.

Abbreviations

The following abbreviations are used in this manuscript:

WSS	Water Supply System
WDN	Water Distribution Network
MILP	Mixed Integer Linear Programming
MINLP	Mixed Integer Nonlinear Programming
BEA	Binary Expansion Approach
SL	Semi-Linear model
FF	Fixed Flow model
Res	Policy of the minimum water tank and reservoir levels
Pol	Policy of turning off the pumps between 6 and 10 p.m.

References

1. COCHILCO. Proyección de consumo de agua en la minería del cobre 2019–2030. Technical Report, Chile. 2019. Available online: https://www.cochilco.cl/Listado%20Temtico/proyeccion%20agua%20mineria%20del%20cobre%202019-2030%20VF.pdf (accessed on 17 July 2024).
2. Herrera-León, S.; Lucay, F.A.; Cisternas, L.A.; Kraslawski, A. Applying a multi-objective optimization approach in designing water supply systems for mining industries. The case of Chile. *J. Clean. Prod.* **2019**, *210*, 994–1004. [CrossRef]
3. Alvez, A.; Aitken, D.; Rivera, D.; Vergara, M.; McIntyre, N.; Concha, F. At the crossroads: Can desalination be a suitable public policy solution to address water scarcity in Chile's mining zones? *J. Environ. Manag.* **2020**, *258*, 110039. [CrossRef]
4. Goldstein, R.; Smith, W. *Water and Sustainability: U.S. Electricity Consumption for Water Supply and Treatment—The Next Half Century*; Technical Report; EPRI: Palo Alto, CA, USA, 2002; Volume 4.
5. Klein, G.; Krebs, M. *California's Water—Energy Relationship*; Technical Report November; California Energy Commission: Sacramento, CA, USA, 2005.
6. Ghaddar, B.; Naoum-Sawaya, J.; Kishimoto, A.; Taheri, N.; Eck, B. A Lagrangian decomposition approach for the pump scheduling problem in water networks. *Eur. J. Oper. Res.* **2015**, *241*, 490–501. [CrossRef]
7. Government of Chile. Ministro de Energía anuncia que "para el 2025 habremos retirado el 50% de las centrales a carbón". Chile, 2021. Available online: https://www.gob.cl/noticias/ministro-de-energia-anuncia-que-para-el-2025-habremos-retirado-el-50-de-las-centrales-a-carbon/ (accessed on 17 July 2024).
8. Garreaud, R.D.; Boisier, J.P.; Rondanelli, R.; Montecinos, A.; Veloso-Aguila, H.H.S.D. The Central Chile Mega Drought (2010–2018): A climate dynamics perspective. *Int. J. Climatol.* **2020**, *40*, 421–439. [CrossRef]
9. Vicuña, S.; Gil, M.; Melo, O.; Donoso, G.; Merino, P.; Vicuña, S.; Gil, M.; Melo, O.; Donoso, G.; Merino, P.; et al. Water option contracts for climate change adaptation in Santiago, Chile. *Water Int.* **2018**, *43*, 237–256. [CrossRef]
10. Herrera, S.; Cisternas, L.A.; Gálvez, E.D. Simultaneous Design of Desalination Plants and Distribution Water Network. *Comput. Aided Chem. Eng.* **2015**, *37*, 1193–1198. [CrossRef]
11. De la perrière, L.B.; Jouglet, A.; Nace, D. Optimisation de la Gestion des Réseaux d'eau Potable par la Programmation Linéaire en Nombre Entiers. Ph.D. Thesis, Université de Technologie de Compiègne, Compiègne, France, 2011.
12. D'Ambrosio, C.; Lodi, A.; Wiese, S.; Bragalli, C. Mathematical programming techniques in water network optimization. *Eur. J. Oper. Res.* **2015**, *243*, 774–788. [CrossRef]
13. Abdallah, M.; Kapelan, Z. Fast Pump Scheduling Method for Optimum Energy Cost and Water Quality in Water Distribution Networks with Fixed and Variable Speed Pumps. *J. Water Resour. Plan. Manag.* **2019**, *145*, 1–13. [CrossRef]
14. Sherali, H.D.; Smith, E.P.; Kim, S.i. A Pipe Reliability and Cost Model for an Integrated Approach Toward Designing Water Distribution Systems. *Glob. Optim. Eng. Des.* **1996**, *9*, 333–354. [CrossRef]
15. Bragalli, C.; D'Ambrosio, C.; Lee, J.; Lodi, A.; Toth, P. On the optimal design of water distribution networks: A practical MINLP approach. *Optim. Eng.* **2012**, *13*, 219–246. [CrossRef]

16. Sherali, H.D.; Subramanian, S.; Loganathan, G.V. Effective Relaxations and Partitioning Schemes for Solving Water Distribution Network Design Problems to Global Optimality. *J. Glob. Optim.* **2001**, *19*, 1–26. [CrossRef]
17. Eiger, G.; Shamir, U.; Ben-Tal, A. Optimal Design of Water Distribution Networks. *Water Resour. Res.* **1994**, *30*, 2637–2646. [CrossRef]
18. Ormsbee, L.; Lansey, K. Optimal Control of Water Supply Pumping Systems. *Water Resour. Plan. Manag.* **1994**, *122*, 322–386. [CrossRef]
19. Nitivattananon, V.; Sadowski, E.; Quimpo, R. Optimization of Water Supply System Operation. *Water Resour. Plan. Manag.* **1996**, *122*, 374–384. [CrossRef]
20. van Zyl, J.E.; Savic, D.A.; Walters, G.A. Operational Optimization of Water Distribution Systems Using a Hybrid Genetic Algorithm. *J. Water Resour. Plan. Manag.* **2004**, *130*, 160–170. [CrossRef]
21. Dreizin, Y. Examination of Possibilities of Energy Saving in Regional Water Supply Systems. Ph.D. Thesis, Technion-Israel Institute of Technology, Haifa, Israel, 1970.
22. Sterling, M.; Coulbeck, B. A dynamic programming solution to optimization of pumping costs. *Proc. Inst. Civ. Eng.* **1975**, *59*, 813–818. [CrossRef]
23. Zessler, U.; Shamir, U. Optimal Operation of Water Distribution Systems. *J. Water Resour. Plan. Manag.* **1989**, *115*, 735–752. [CrossRef]
24. Coulbeck, B.; Brdys, M.; Orr, C.H.; Rance, J.P. A hierarchical approach to optimized control of water distribution systems: Part II. Lower-level algorithm. *Optim. Control Appl. Methods* **1988**, *9*, 109–126. [CrossRef]
25. Coulbeck, B.; Brdys, M.; Orr, C.H.; Rance, J.P. A hierarchical approach to optimized control of water distribution systems: Part I decomposition. *Optim. Control Appl. Methods* **1988**, *9*, 51–61. [CrossRef]
26. Fallside, F.; Perry, P.F. Hierarchial model for water-supply-system control. *Proc. IEEE* **1975**, *122*, 441–443. [CrossRef]
27. Sterling, M.; Coulbeck, B. Optimisation of water pumping costs by hierarchical methods. *Proc. Inst. Civ. Eng.* **1975**, *59*, 789–797. [CrossRef]
28. Alperovits, E.; Shamir, U. Design of optimal water distribution systems. *Water Resour. Res.* **1977**, *13*, 885–900. [CrossRef]
29. Schwarz, J.; Meidad, N.; Shamir, U. Water quality management in regional systems. *Water Resour. Manag.* **1985**, *153*, 341–349.
30. Ormsbee, L.E.; Walski, T.M.; Chase, D.V.; Sharp, W.W. Methodology for improving pump operation efficiency. *J. Water Resour. Plan. Manag.* **1989**, *115*, 148–164. [CrossRef]
31. Maier, H.R.; Kapelan, Z.; Kasprzyk, J.; Kollat, J.; Matott, L.S.; Cunha, M.C.; Dandy, G.C.; Gibbs, M.S.; Keedwell, E.; Marchi, A.; et al. Evolutionary algorithms and other metaheuristics in water resources: Current status, research challenges and future directions. *Environ. Model. Softw.* **2014**, *62*, 271–299. [CrossRef]
32. Nicklow, J.; Reed, P.; Savic, D.; Dessalegne, T.; Harrell, L.; Chan-Hilton, A.; Karamouz, M.; Minsker, B.; Ostfeld, A.; Singh, A.; et al. State of the Art for Genetic Algorithms and Beyond in Water Resources Planning and Management. *J. Water Resour. Plan. Manag.* **2010**, *136*, 412–432. [CrossRef]
33. Creaco, E.; Pezzinga, G. Embedding linear programming in multi objective genetic algorithms for reducing the size of the search space with application to leakage minimization in water distribution networks. *Environ. Model. Softw.* **2015**, *69*, 308–318. [CrossRef]
34. Derceto. Derceto Aquadapt, About Us Web Page. Available online: https://www.suezsmartsolutions.com/about-us (accessed on 17 July 2024).
35. Rossman, L.S. EPANET, Web Page. Available online: https://www.epa.gov/water-research/epanet (accessed on 17 July 2024).
36. Morsi, A.; Geißler, B.; Martin, A. Mixed Integer Optimization of Water Supply Networks. In *Mathematical Optimization of Water Networks. International Series of Numerical Mathematics*; Birkhäuser: Basel, Switzerland, 2012; Volume 162.
37. Verleye, D.; Aghezzaf, E.H. Generalized Benders Decomposition to Reoptimize Water Production and Distribution Operations in a Real Water Supply Network. *J. Water Resour. Plan. Manag.* **2016**, *142*, 04015059. [CrossRef]
38. Burgschweiger, J.; Gnädig, B.; Steinbach, M.C. Optimization models for operative planning in drinking water networks. *Optim. Eng.* **2009**, *10*, 43–73. [CrossRef]
39. Fooladivanda, D.; Taylor, J.A. Energy-optimal pump scheduling and water flow. *IEEE Trans. Control Netw. Syst.* **2018**, *5*, 1016–1026. [CrossRef]
40. Fugenschuh, A.; Humpola, J. *A Unified View on Relaxations for a Nonlinear Network Flow Problem*; Technical Report July; Zuse Institut Berlin: Berlin, Germany, 2013.
41. Gurobi. General Constraints Page. Available online: https://www.gurobi.com/documentation/current/refman/general_constraints.html (accessed on 17 July 2024).
42. Herrera-León, S.; Kraslawski, A.; Cisternas, L.A. A MINLP model to design desalinated water supply systems including solar energy as an energy source. In *Computer Aided Chemical Engineering*; Elsevier: Amsterdam, The Netherlands, 2018; Volume 44. [CrossRef]
43. Meng, F.; Fu, G.; Farmani, R.; Sweetapple, C.; Butler, D. Topological attributes of network resilience: A study in water distribution systems. *Water Res.* **2018**, *143*, 376–386. [CrossRef] [PubMed]
44. Basupi, I.; Kapelan, Z. Evaluating Flexibility in Water Distribution System Design under Future Demand Uncertainty. *J. Infrastruct. Syst.* **2015**, *21*, 04014034. [CrossRef]

45. Menke, R.; Abraham, E.; Parpas, P.; Stoianov, I. Demonstrating demand response from water distribution system through pump scheduling. *Appl. Energy* **2018**, *170*, 377–387. [CrossRef]
46. Oikonomou, K.; Parvania, M.; Khatami, R. Optimal Demand Response Scheduling for Water Distribution Systems. *IEEE Trans. Ind. Inform.* **2018**, *14*, 5112–5122. [CrossRef]
47. Mkireb, C.; Dembele, A.; Denoeux, T.; Jouglet, A. Flexibility of drinking water systems: An opportunity to reduce CO2 emissions. *Int. J. Energy Prod. Manag.* **2019**, *4*, 134–144. [CrossRef]
48. Stuhlmacher, A.; Mathieu, J.L. Chance-Constrained Water Pumping to Manage Water and Power Demand Uncertainty in Distribution Networks. *Proc. IEEE* **2020**, *108*, 1640–1655. [CrossRef]
49. Zhou, X.; Zhang, H.; Qiu, R.; Liang, Y.; Wu, G.; Xiang, C.; Yan, X. A hybrid time MILP model for the pump scheduling of multi-product pipelines based on the rigorous description of the pipeline hydraulic loss changes. *Comput. Chem. Eng.* **2019**, *121*, 174–199. [CrossRef]
50. Herrera-León, S.; Lucay, F.; Kraslawski, A.; Cisternas, L.A.; Gálvez, E.D. Optimization Approach to Designing Water Supply Systems in Non-Coastal Areas Suffering from Water Scarcity. *Water Resour. Manag.* **2018**, *32*, 2457–2473. [CrossRef]
51. Bhave, P.; Gupta, R. *Analysis of Water Distribution Networks*; Alpha Science International: Oxford, UK, 2006.
52. Li, Q.; Yu, S.; Al-Sumaiti, A.S.; Turitsyn, K. Micro water-energy nexus: Optimal demand-side management and quasi-convex hull relaxation. *IEEE Trans. Control Netw. Syst.* **2019**, *6*, 1313–1322. [CrossRef]
53. Lansey, K.E.; Awumah, K. Optimal Pump Operations Considering Pump Switches. *J. Water Resour. Plan. Manag.* **1994**, *120*, 17–35. [CrossRef]
54. Savic, D.; Walters, G.; Schwab, M. Multiobjective genetic algorithms for pump scheduling in water supply. In *Evolutionary Computing. Lecture Notes in Computer Science*; Springer: Berlin/Heidelberg, Germany, 1997; Volume 1305. [CrossRef]
55. Menke, R.; Abraham, E.; Parpas, P.; Stoianov, I. Approximation of system components for pump scheduling optimisation. *Procedia Eng.* **2015**, *119*, 1059–1068. [CrossRef]
56. Gunluk, O.; Lee, J.; Leung, J. A Polytope for a Product of Real Linear Functions in 0/1 Variables. In *Mixed Integer Nonlinear Programming. The IMA Volumes in Mathematics and Its Applications*; Springer: New York, NY, USA, 2012; Volume 154, pp. 513–529. [CrossRef]
57. Tapia, T.; Lorca, Á.; Olivares, D.; Negrete-Pincetic, M.; Lamadrid L, A.J. A robust decision-support method based on optimization and simulation for wildfire resilience in highly renewable power systems. *Eur. J. Oper. Res.* **2021**, *294*, 723–733. [CrossRef]
58. Gurobi Optimization. Gurobi Optimizer Reference Manual Page. Available online: https://www.gurobi.com (accessed on 17 July 2024).
59. Julia. The Julia Programming Language. Available online: https://julialang.org/ (accessed on 17 July 2024).
60. SGA—Soluciones Ambientales. Estudio Impacto Ambiental Proyecto RT Sulfuros CODELCO-CHILE. Technical report, Chapter 1. 2013. Available online: https://www.idbinvest.org/sites/default/files/2018-10/EIA%20Desaladora%20RT%20Cap%2001%20Descripcion%20del%20Proyecto-ilovepdf-compressed.pdf (accessed on 17 July 2024).